A VLA SURVEY OF STRONG RADIO SOURCES

J. ULVESTAD a) AND K. JOHNSTON

E. O. Hulburt Center for Space Research, Naval Research Laboratory, Washington, D.C. 20375

R. PERLEY AND E. FOMALONT

National Radio Astronomy Observatory, ^{b)} Socorro, New Mexico 87801 Received 16 January 1981; revised 9 April 1981

ABSTRACT

The VLA has been used to survey the structures of 360 strong high-frequency radio sources at 1480 and 4900 MHz. Of those sources, 250 are found to contain at least 90% of their flux density in an unresolved component (≤ 1 arcsec), while the remaining 110 sources are considered to be resolved. Positions and structural information for these sources are given, and maps of 20 of the resolved objects are shown. The VLA data have been combined with other structural information available for sources listed in the Parkes and S surveys in order to study a complete sample of 444 extragalactic objects having flux densities greater than 1 Jy at 5 GHz. The unresolved radio sources in the flux-limited sample have a median spectral index of $\alpha = -0.09$ ($S_{\nu} \sim \nu^{\alpha}$) at centimeter wavelengths, while the resolved sources have a median index of $\alpha = -0.73$. The unresolved radio galaxies, in general, have steeper spectra than both the resolved and the unresolved quasars. Finally, there seems to be a lack of quasars having radio sources with large linear diameters beyond $z \simeq 1$.

I. INTRODUCTION

We have used the partially completed Very Large Array (VLA) to conduct a survey of the structure of strong extragalactic radio sources. The sources were selected from the S surveys made at 5 GHz (Pauliny-Toth *et al.* 1978 and references therein) and the Parkes 2.7-GHz surveys (Savage, Bolton, and Wright 1977 and references therein). These surveys are virtually complete for sources having flux densities greater than ~ 0.6 Jy at 5 GHz and lying more than 10° from the galactic plane. Figure 2 of Pauliny-Toth *et al.* (1978) gives an outline of the surveyed regions.

Two basic criteria were used in selecting sources for our observations. First, we chose objects whose 5-GHz flux densities were reported to be greater than 1 Jy in the surveys mentioned above. Since many strong extragalactic sources are variable, this constraint does not mean that all our sources exceeded the flux density limit at the time of our observations. Second, we attempted to choose sources for which no high-resolution maps (e.g., Cambridge 5-km telescope maps) were available in the literature. The first criterion was relaxed for ~25 objects in order to fill in gaps in the observing program, while the second criterion was ignored for a few well-known sources that we observed as a test to ensure that our reduction methods gave correct results.

The results of our study are given in the text and ta-

bles in the following sections. In Sec. II, we describe our VLA observations, tabulate the new data, and present maps of some of the more interesting sources. Then, in Sec. III, we construct a complete sample of high-frequency radio sources and present some analysis of the properties of that sample. Finally, Sec. IV contains a summary of our major conclusions.

II. VLA OBSERVATIONS AND RESULTS

We observed a total of 288 sources, including calibrators, on the partially constructed VLA during the period 3–6 February 1979. The telescope was divided into two sub-arrays operating in parallel at frequencies of 1480 and 4900 MHz (20- and 6-cm wavelength, respectively). Seven antennas were used in each sub-array, with spacings ranging from 100 m to 13.6 km at the lower frequency and 1 to 15 km at the higher frequency. The longest spacings gave resolutions of $\sim 3''$ at 1480 MHz and $\sim 0''.8$ at 4900 MHz. Almost all sources were observed at a minimum of three hour angles. However, scheduling problems, holes in our observing run, and unusable data limited a small number of sources to two

TABLE I. Source scans in various declination bands.

Declination range	No. of observations
50° to 70°	8
40° to 50°	7
30° to 40°	6
10° to 30°	5
- 10° to 10°	4
— 45° to — 10°	3

^{a)}Also with Astronomy Program, University of Maryland, College Park, Maryland 20742. NRAO summer student, 1978.

1010 Astron. J. 86(7), July 1981

0004-6256/81/071010-26\$00.90

© 1981 Am. Astron. Soc.

1010

^{b)}Operated by Associated Universities, Inc., under contract with the National Science Foundation.

TABLE II. Calibration sources in VLA survey.

Source	1480 MHz	nsity (Jy)	
		4900 MHz	,
0201 + 113	1.01 P	1.00 P	
0202 + 319	0.85		
0235 + 164	1.53		
0237 - 233		3.07 P	
0316 + 161		2.65 P	
0319 + 121	1.70		
0400 + 258	1.65		
0420 - 014		2.99	
0426 - 380		1.08	
0428 + 205	3.80	1.00	
0457 + 024	1.40		
0500 + 019	2.25		
0518 + 165	8.62 P		
0528 - 250	1.12		
0528 + 134		2.50 P	
0552 + 398	1.72 P	4.81 P	
0711 + 356		1.14	
0727 - 115		3.19 P	
0738 + 313	2.10	5.171	
0742 + 103	3.70 P	4.00 P	
0748 + 126	1.63	4.001	
0826 - 373	1100	4.01	
0919 - 260		2.37	
1117 + 146	2.35	2.37	
1127 - 145	2.33	4.75 P	
1155 - 251	1.03 P	0.91 P	
1245 - 197	5.14 P	2.34 P	
1252 + 119	1.08 P	1.04	
1311 + 678	1.001	0.86	
1323 + 321	4.65	0.80	
1328 + 254	6.91 P	3.17 P	
1328 + 307	14.44 P	7.41 P	
1511 + 238	1.63	7.41 1	
1519 - 273	1.03	1.35	
1555 + 001	1.46 P	1.26	
1607 + 268	4.75	1.20	
1741 - 038	1.91 P	2.24	
2005 + 403	3.49 P	3.73 P	
2128 + 048	3.85	3./3 F	
2128 - 123	5.05	2.45	
2134 + 004		9.72	
2200 + 420	2.10 P		
2234 + 282	0.90	1.73 P	
2352 + 495	2.60 P	1.57 P	
	2.001	1.37 P	

observations or, in rare cases, only one observation. Table I shows the approximate number of scans made as a function of source declination. Individual scans were 2–3 min in length, a time adequate to establish a sufficient signal-to-noise ratio for the strong sources, and were scheduled in order to maximize the u-v plane coverage in each declination band.

The interferometer phases and amplitudes were calibrated using the sources listed in Table II. In that table, column 1 gives the calibrator's IAU name and column 2 gives the initially assumed flux density in Jansky at 1480 MHz (*L*-band) for all sources used as calibrators at that frequency. The letter P denotes primary calibrators, objects for which VLA survey observations show no resolution on our baselines. Column 3 gives the initial assumed flux densities for sources used as calibrators at 4900 MHz, with the letter P having the same meaning as in column 2.

Maps of all sources were made at 4900 MHz in order

to establish their positions relative to the primary calibrators, whose positions are known with an accuracy of \sim 0".1. After the positions of all sources were derived, both the primary and secondary calibrators were used in the final calibration of the data. The amplitude scale was set by adopting the flux density of 3C 286 (1328 + 307) as 14.44 and 7.41 Jy at 1480 and 4900 MHz, respectively (from scale of Baars *et al.* 1977).

The sources showing less than 10% of their total flux density in extended emission or secondary components were considered unresolved; those sources are listed in Table III. In addition to the sources studied during February 1979, Table III also contains all sources observed in the VLA calibration program by mid-1980 which have been found to have little or no resolved structure at \sim 1465 and \sim 4885 MHz. Not all of these sources have flux densities above 1 Jy at 5 GHz, but we report them here for the purposes of providing information to other radio observers. The subset of sources in Table III with observed 5-GHz flux densities above 1 Jy is a sample of unresolved radio sources, which we estimate to be $\gtrsim 90\%$ complete at a given time for declinations between $+70^{\circ}$ and -45° (excluding regions where |b|10°). This estimate is based on the fact that we have not observed 18 sources in the flux-limited sample, while 250 unresolved sources are listed in Table III (the surveys from which our sources have been drawn are estimated by their authors to be virtually complete to flux density limits below 1 Jy). A few sources having δ > + 70° are included in Table III, but that part of the list is far from being complete, since the S surveys from which the northern sources were drawn were not published at the time this research was conducted.

In Table III, column 1 gives the IAU source designation, while column 2 gives an alternative 3C or 4C name. Column 3 gives an optical identification (GAL = galaxy, QSS = quasi-stellar source) taken from references listed in the Appendix. Columns 4 and 5 give the 1950 epoch right ascension and declination, with positional accuracies \leq 0"2 for VLA calibrators and \leq 0"4 in most other cases. The source flux densities at 20, 6, and (where applicable) 2 cm are given in columns 6–8, respectively. For sources or frequencies not observed in the main survey, these values are taken from calibration runs made as close as possible in time to February 1979. Finally, column 9 specifies the sources which are VLA calibrators, with the letters L, C, and U denoting calibrators at 20, 6, and 2 cm, respectively.

All sources displaying structure were mapped at 1480 MHz. No maps at 4900 MHz were made for presentation because our minimum antenna spacing of 1 km at that frequency made the observations insensitive to structures $\gtrsim 12''$. Parameters for these resolved sources are listed in Table IV. Columns 1–3 give information similar to that listed in Table III. Columns 4 and 5 give 1950 epoch right ascensions and declinations, with positional accuracies of $\lesssim 1''$. For sources with a single resolved component, the position refers to the radio peak,

TABLE III. Unresolved sources. a

Source	Other Name	Optical ID	$^{\alpha}$ (1950)	^δ (1950)	S ₂₀	⁸ 6	s ₂	VLA
0003-066		GAL	00 ^h 03 ^m 40.29	-06°40'17 " 3	1.5	1.5		L,C
0007+171		QSS	00 07 59.38	+17 07 37.5	0.8	0.9	1.0	L,C
0008-421		GAL	00 08 21.36	-42 09 52.3	3.6	1.1		L,C
0016+731		QSS	00 16 54.20	+73 10 51.5	1.1	1.7	1.5	L,C
0019-000	4C+00.02	GAL	00 19 51.65	-00 01 41.7	2.9	1.1		L,C
0022-423			00 22 15.42	-42 18 40.7	2.8	1.5		
0026+346			00 26 34.84	+34 39 57.6	2.0	1.2		
0056-001	4C-00.06	QSS	00 56 31.758	-00 09 18.7	2.5	1.4	1.5	L,C
0108+388			01 08 47.26	+38 50 32.8	0.5	1.2		
0112-017		QSS	01 12 43.92	-01 42 55.0	0.9	0.9		
0116+319	4C+31.04	GAL	01 16 47.245	+31 55 05.78	2.6	1.5	1.2	L,C
0119+041		QSS	01 19 21.39	+04 06 44.0	1.2	1.1		L,C
0133+476		QSS	01 33 55.11	+47 36 12.8	1.6	2.0		L,C
0134+329	3C48	QSS	01 34 49.832	+32 54 20.52	15.2		2.9	L,C
0135-247		QSS	01 35 17.11	-24 46 08.7	1.0	0.7		
0138-097		QSS	01 38 56.86	-09 43 51.7	0.5	1.2		
0146+056		QSS	01 46 45.53	+05 41 00.7	0.6	0.9		L,C
0149+218		QSS	01 49 31.75	+21 52 20.9	1.2	1.4		L,C
0150-334		QSS	01 50 57.01	-33 25 10.7	0.9	0.7		L,C
0153+744		QSS	01 53 04.35	+74 28 05.7	1.8	1.1		L,C
0201+113		GAL	02 01 05.98	+11 20 22.9	1.0	1.1		L,C
0202+319		QSS	02 02 09.66	+31 58 10.4	1.0	1.2		L,C
0202+149	4C+15.05		02 02 07.40	+14 59 51.0	3.9	2.9	0.4	L,C
0202-172		QSS	02 02 34.52	-17 15 39.4	1.3	1.2		
0212+735		QSS	02 12 49.93	+73 35 40.2	2.4	2.2	2.9	L,C
0221+067	4C+06.11	QSS	02 21 49.96	+06 45 50.4	0.5	0.7		, -
0223+341	4C+34.07		02 23 09.74	+34 08 01.5	2.5			
0224+671	. 4C+67.05	QSS	02 24 41.17	+67 07 39.7	1.0	1.5	1.4	С
0235+164		QSS	02 35 52.63	16 24 03.93	1.6	1.4		L,C
0237-027		QSS	02 37 13.71	-02 47 32.8	0.3	0.9		C
0237-233		QSS	02 37 52.80	-23 22 06.4	6.7	3.3		L,C
0248+430		QSS	02 48 18.49	+43 02 57.0	0.7	1.3	1.3	
0256+075		QSS	02 56 47.00	+07 35 45.2	1.1	0.8		-
0316+161	3C83.1		03 16 09.14	+16 17 40.4	7.7	2.9		L,C
0316+413	3C84	GAL	03 16 29.565	+41 19 51.90	14.2	56.	50.	C C
0319+121		QSS	03 19 08.22	+12 10 31.5	1.8	1.1		L,C
0332+078			03 32 12.13	+07 50 10.4	0.4	0.5		L,C
0332-403		QSS	03 32 25.24	-40 18 23.9	1.1	1.5		L,C
0333+321	4C+32.14	QSS	03 33 22.408	+32 08 36.62	3.4	2.4	2.2	L,C
0336-019		QSS	03 36 58.957	-01 56 16.97	2.2	2.6	4.1	L,C
0355+508		~ -	03 55 45.261	+50 49 20.29	5.6	11.2	15.0	-,0
0400+258		QSS	04 00 03.60	+25 51 46.5	1.6	1.2		L,C
0406+121			04 06 35.48	+12 09 49.3	1.0	1.2		L,C

TABLE III. (continued)

Source	Other Name	Optical ID	^α (1950)	^δ (1950)	S ₂₀	s ₆	s ₂	VLA
0420-014		QSS	04 20 43.54	-01 27 28.7	1.0	3.1		L,C
0426-380		QSS	04 26 54.72	-38 02 52.1	0.9	1.2		L,C
0428+205*	*	GAL	04 28 06.87	+20 31 09.1	3.8	2.3		L,C
0429+415*	* 3C119	QSS	04 29 07.90	+41 32 08.5	8.3	3.5	2.4	Ĺ
0430+052*	* 3C120	GAL	04 30 31.60	+05 14 59.5	6.7	3.3	4.3	U
0438-436*		QSS	04 38 43.18	-43 38 53.2	5.3	3.9	2.1	L,C
0440-003*	*	QSS	04 40 05.29	-00 23 20.5	2.3	1.5		
0454+844			04 54 57.14	+84 27 53.1	0.8	1.6	2.3	L,C,U
0454-234		QSS	04 54 57.32	-23 29 29.1	1.5	2.3		
0457+024		QSS	04 57 15.55	+02 25 05.7	1.8	1.2		L,C
0458-020	4C-02.19	QSS	04 58 41.34	-02 03 33.4	1.7	1.9		
0500+019			05 00 45.16	+01 58 53.9	2.4	2.0		L,C
0528-250		QSS	05 28 05.20	-25 05 44.5	1.1	0.8		L,C
0528+134		QSS	05 28 06.75	+13 29 42.2	1.5	2.5		L,C
0531+194*	**	GAL	05 31 47.36	+19 25 24.7	6.6	2.4		L,C
0537-441		QSS	05 37 21.07	-44 06 45	3.2	4.2		С
0552+398		QSS	05 52 01.409	+39 48 21.94	1.6	4.7	3.0	L,C
0602+673			06 02 38.89	+67 21 18.5	0.6	0.7		L,C
0606-223		QSS	06 06 53.38	-22 19 46.2	0.9	0.8		
0607-157		QSS	06 07 26.02	-15 42 02.5	1.8	2.4		С
0615+820		QSS	06 15 32.77	+82 03 56.5	0.7	1.0		C
0642+449		QSS	06 42 53.00	+44 54 30.9	0.9	0.7		L,C
0646+600			06 46 04.12	+60 05 14.2	0.5	0.9		С
0648-165			06 48 10.31	-16 34 05.9	1.7	2.2		
0710+439		GAL	07 10 03.37	+43 54 26.0	2.1	1.6		
0711+356		QSS	07 11 05.60	+35 39 52.5	1.7	1.2		
0723-008		GAL	07 23 17.84	-00 48 55.4	2.2	1.8		
0727-115			07 27 58.10	-11 34 52.6	2.1	3.0	3.5	L,C,U
0733-174			07 33 31.41	-17 29 06.2	2.9	1.9		
0735+178		QSS	07 35 14.13	+17 49 09.3	1.9	2.1		С
0736+017		QSS	07 36 42.51	+01 44 00.2	2.5	2.2		
0738+313		QSS	07 38 00.19	+31 19 02.1	2.1	1.6		L,C
0742+103			07 42 48.67	+10 18 32.6	3.5	3.6	2.0	L,C,U
0743-006	4C-00.28	QSS	07 43 21.01	-00 36 55.7	0.9	1.3		С
0748+126		QSS	07 48 05.06	+12 38 45.3	1.7	1.5		L,C
0804+499		QSS	08 04 58.40	+49 59 23.1	0.8	1.1		С
0814+425		QSS	08 14 51.672	+42 32 07.68	1.3	1.6	1.4	С
0823+033		QSS	08 23 13.53	+03 19 15.3	1.2	1.0		L,C
0823-223		QSS	08 23 50.07	-22 20 34.8	2.0	2.8		L,C
0826-373			08 26 12.04	-37 21 06.1	1.8	5.0	2.7	L,C
0828+493		QSS	08 28 47.95	+49 23 33.1	1.4	1.5		L,C
0831+557*	* 4C+55.16	GAL	08 31 04.381	+55 44 41.36	7.9	5.5	2.5	С
0833+585		QSS	08 33 23.77	+58 35 30.2	0.5	1.2		

TABLE III. (continued)

Source	Other Name	Optical ID	^α (1950)	^δ (1950)	s ₂₀	s ₆	s ₂	VLA
0834-201		QSS	08 34 24.60	-20 06 30.4	3.0	1.9	0.9	С
0834-196			08 34 56.15	-19 41 25.4	4.6	1.4		
0836+710	4C+71.07	QSS	08 36 21.54	+71 04 22.4	3.9	2.5	1.1	L,C,U
0839+187		QSS	08 39 14.09	+18 46 27.3	1.3	1.0		L,C
0851+202		QSS	08 51 57.253	+20 17 58.39	1.7	2.8	2.4	L,C
0859+681		QSS	08 59 23.04	+68 09 16.1	0.6	0.4		L,C
0859-140		QSS	08 59 54.95	-14 03 38.8	3.0	2.1	*	
0906+015	4C+01.24	QSS	09 06 35.20	+01 33 47.3	0.7	1.4		С
0917+624		QSS	09 17 40.30	+62 28 38.7	1.1	1.2	2.1	C,U
0917+449		QSS	09 17 41.92	+44 54 39.6	0.6	0.8	2.5	С
0919-260		QSS	09 19 16.71	-26 05 54.5	1.1	2.1	2.7	L,C
0922+005		QSS	09 22 33.77	+00 32 12.2	0.9	0.7		С
0941-080		GAL	09 41 08.64	-08 05 44.1	2.6	1.0		
0954+658		QSS	09 54 57.85	+65 48 15.6	0.5	0.6		С
0955+476		QSS	09 55 08.53	+47 39 28.2	0.6	0.9		С
1004-018*	***	QSS	10 04 31.69	-01 52 30.8	0.5	0.5		L,C
1015+359		QSS	10 15 16.22	+35 57 41.3	0.8	0.7		С
1015-314			10 15 53.39	-31 29 11.3	3.5	1.3	0.7	L,C
1030+415			10 30 07.82	+41 31 34.4	0.7	0.6		
1031+567		GAL	10 31 55.97	+56 44 18.1	1.9	1.2	0.8	L,C
1032-199		QSS	10 32 37.36	-19 56 02.2	1.1	0.9		
1034-293		QSS	10 34 55.86	-29 18 27.0	1.1	1.9		С
1117+146	4C+14.41	QSS	11 17 50.97	+14 37 21.1	2.3	1.1		L,C
1127-145		QSS	11 27 35.68	-14 32 54.4	6.2	4.7	2.5	L,C,U
1143-245		QSS	11 43 36.38	-24 30 52.9	1.5	1.1		C
1144+542		QSS	11 44 04.57	+54 13 22.9	0.6	0.6		С
1145-071		QSS	11 45 18.30	-07 08 00.8	1.0	1.0		
1148-001	4C-00.47	QSS	11 48 10.12	-00 07 13.3	2.8	1.9		L,C
1150+812		QSS	11 50 23.49	+81 15 10.2	1.4	1.2	1.3	С
1151-348*	*	QSS	11 51 49.44	-34 48 47.2	5.2	2.5		L,C
1155+251		GAL	11 55 51.64	+25 06 59.8	1.0	0.9		L,C
1213+350	4C+35.28	QSS	12 13 24.83	+35 04 54.9	1.4	0.9	0.5	
1216+487		QSS	12 16 38.58	+48 46 34.9	0.8	1.0	1.0	C
1236+077		QSS	12 36 52.3	+07 46 45.4	0.6	0.7		
1237-101		QSS	12 37 07.28	-10 07 00.7	1.5	1.0		
1243-072		QSS	12 43 28.79	-07 14 23.5	0.8	1.4		L,C
1245-197			12 45 45.22	-19 42 57.5	5.4	2.3	1.2	L,C,U
1250+568	3C277.1	QSS	12 50 15.23	+56 50 36.1	2.2	0.7		
1252+119		QSS	12 52 07.71	+11 57 20.7	1.1	1.0	1.5	L,C,U
1255-316		QSS	12 55 15.18	-31 39 05.1	1.1	1.0		L,C
1257+145		QSS	12 57 51.55	+14 33 27.3	0.6	0.4		
1302-102		QSS	13 02 55.85	-10 17 16.5	0.6	1.0		

TABLE III. (continued)

Source	Other Name	Optical ID	^α (1950)	^δ (1950)	s ₂₀	s ₆	s ₂	VLA
1308+326		QSS	13 08 07.56	+32 36 40.2	1.5	2.5		
1308-220	3C283	GAL	13 08 57.4	-22 00 46.7	5.1	1.1		
1311+678	4C+67.22		13 11 45.06	+67 51 42.2	2.4	0.9	0.9	L,C
1313+200		QSS	13 13 58.57	+20 02 52.9	0.4	0.3		
1320-446**	+		13 20 07.40	-44 36 53.4	3.1	1.0		
1323+321	4C+32.44	GAL	13 23 57.9	+32 09 43.0	4.7	2.3		L,C
1323+799			13 23 30.98	+79 58 27.5	0.4	0.6		L,C
1328+254	3C287	QSS	13 28 15.93	+25 24 37.5	7.0	3.2	1.8	L,C,U
1328+307	3C286	QSS	13 28 49.66	+30 45 58.6	14.5	7.4	3.5	L,C,U
1334-127		QSS	13 34 59.82	-12 42 09.9	1.6	1.9	3.5	С
1345+125	4C+12.50	GAL	13 45 06.17	+12 32 20.3	5.0	2.7		
1351-018			13 51 32.03	-01 51 20.0	0.8	0.9		
1354-152		QSS	13 54 28.59	-15 12 51.8	1.0	1.5		L,C
1354+195	4C+19.44	QSS	13 54 42.09	+19 33 44.0	1.4	1.8		
1357+769		QSS	13 57 42.12	+76 57 53.3	0.6	0.7	0.9	С
1358+624**	4C+62.22	GAL	13 58 58.36	+62 25 06.6	4.3	1.7		L,C
1402-012		QSS	14 02 11 29	-01 16 01.8	0.7	0.7		L,C
1402+044		QSS	14 02 29.97	+04 29 55.6	0.6	0.7		
1402+660**	4C+66.14		14 02 48.41	+66 05 57.4	1.9	0.7	0.7	L
1404+286		GAL	14 04 45.62	+28 41 29.2	0.8	3.0	0.9	L,C
1413+135		QSS	14 13 33.90	+13 34 17.4	1.1	1.0		С
1413+349		QSS	14 13 56.28	+34 58 29.4	2.0	1.0		
1416+067	3C298	QSS	14 16 38.77	+06 42 20.9	5.3	1.7		
1418+546		QSS	14 18 06.20	+54 36 57.9	0.6	0.7	2.1	L,C
1427+109		QSS	14 27 43.70	+10 56 44.7	0.3	0.8		
1434+235		QSS	14 34 25.40	+23 34 03.2	0.6	0.5		
1435+638		QSS	14 35 37.25	+63 49 35.8	1.2	0.9		
1442+101		QSS	14 42 50.47	+10 11 12.2	2.5	1.1		L,C
1444+175	4C+17.61	QSS	14 44 15.44	+17 33 39.7	0.8	0.8		C
1502+106	4C+10.39	QSS	15 02 00.159	+10 41 17.71	1.9	2.1	2.5	L,C
1504+377**			15 04 12.96	+37 42 23.2	1.2	0.9		•
1504-166		QSS	15 04 16.43	-16 40 59.3	2.2	2.4		
1511+238	4C+23.41	GAL	15 11 28.30	+23 49 43.7	1.6	0.8		L,C
1514-241		\mathtt{GAL}	15 14 45.28	-24 11 22.6	2.6	2.4		_, _
1517+204	3C318	GAL	15 17 50.63	+20 26 53	2.5	0.8		
1519-273		QSS	15 19 37.27	-27 19 29.5	1.1	2.0	1.4	L,C,U
1524-136**	*	QSS	15 24 12.87	-13 40 34.9	2.4	1.1		_,,,,
1546+027		QSS	15 46 58.29	+02 46 06.1	0.7	1.3		
1547+507		QSS	15 47 52.26	+50 47 09.3	0.7	0.7		L,C
1551+130		QSS	15 51 12.03	+13 05 41.4	1.0	0.7		• -
1555+001		QSS	15 55 17.688	+00 06 43.54	1.3	1.2	2.3	L,C
1600+335		QSS	16 00 11.92	+33 35 09.5	2.7	2.1		·- • -
1607+268		QSS?	16 07 09.27	+26 49 18.6	4.6	1.7		L,C
1611+343		QSS	16 11 47.897	+34 20 19.8	2.8	2.2	1.2	L,C
1622-297			16 22 57.25	-29 44 41.2	2.2	1.7	2.2	•

TABLE III. (continued)

Source	Other Name	Optical ID	^α (1950)	^δ (1950)	s ₂₀	^S 6	s ₂	VLA
624+416*	4C+41.32		16 24 18.24	+41 41 23.5	1.9	1.1		
.633+382*	4C+38.41	QSS	16 33 30.62	+38 14 10.0	2.0	1.9		L,C,U
.634+628	3C343.0	QSS	16 34 01.063	+62 51 41.83	4.7	1.5	0.8	L,C
637+574		QSS	16 37 17.43	+57 26 15.8	1.3	1.6	1.6	U
637+626**	3C343.1	GAL	16 37 55.32	+62 40 34.3	4.4	1.2		L
638+124**	4C+12.60	QSS	16 38 27.91	+12 25 46.3	2.0	1.0	0.4	
638+398		QSS	16 38 48.172	+39 52 30.08	0.5	0.4	0.8	
.648+015			16 48 31.58	+01 34 25.7	0.7	0.7		
652+398	4C+39.49	GAL	16 52 11.74	+39 50 25.0	1.5	1.2		
657-261			16 57 47.75	-26 06 32.3	1.2	1.5		L,C
716+686		QSS	17 16 27.82	+68 39 48.3	0.4	0.7		L,C
.717+178		QSS	17 17 00.34	+17 48 08.5	0.6	0.7	1.2	L,C
725+044		QSS	17 25 56.33	+04 29 27.9	0.6	0.8		
730-130		QSS	17 30 13.54	-13 02 45.9	5.7	5.3	5.2	C,U
732+389		GAL	17 32 40.49	+38 59 46.9	0.8	1.3	-	
739+522	4C+51.37	QSS	17 39 29.02	+52 13 10.5	1.4	1.9		L,C
741-038		ΩSS	17 41 20.62	-03 48 49.0	1.7	2.2	3.0	L,C
748-253		1200	17 48 45.80	-25 23 17.4	1.2	0.5		L,C
.749+701**	***		17 49 03.38	+70 06 39.5	1.5	1.2		L,C
1749+096	4C+09.56	QSS	17 49 10.39	+09 39 42.7	0.8	1.6	7.1	C
751+288	10.09.30	QSS	17 51 45.40	+28 48 36.7	0.9	0.8	, • =	C
L751+2441		QSS	17 51 53.71	+44 10 17.8	0.5	0.8		C
L803+784		GAL	18 03 39.18	+78 27 54.2	1.9	2.5		L,C
L821+107		QSS	18 21 41.68	+10 42 43.9	0.9	1.1		L,C
L908-202		,,,,,,,,,,,,,,,,,,,,,,,,,,,,,,,,,,,,,,,	19 08 12.48	-20 11 55.1	2.4	1.9		L,C
1921-293		o s s	19 21 42.22	-29 20 26.1	4.0	6.8	2.2	L,C
1928+738	4C+73.18	QSS	19 28 49.34	+73 51 45.0	3.2	3.0	3.5	L,C
1933-400	40173.10	QSS	19 33 51.11	-40 04 46.8	1.0	0.7		L,C
1936-155		255	19 36 36.03	-15 32 38.9	0.8	1.4		L,C
1954-388		QSS	19 54 39.07	-38 53 13.3	0.8	1.7		L,C
1954-300		QSS	19 58 04.63	-17 57 16.9	0.5	1.2		C C
2000-330		QSS	20 00 13.01	-33 00 12.5	0.4	1.0		L,C
			20 05 59.56	+40 21 01.8	3.4	3.8	37	L,C,U
2005+403		QSS	20 03 39.38	+77 43 58.1	0.7	1.0	5 /	L,C
2007+776		QSS	20 07 20.42	-15 55 38.3	0.6	1.0		L,C
2008-159		QSS		-06 53 01.8		1.2		1,0
2008-068		0.00	20 08 33.70 20 21 13.28		2.6		2 0	T C II
2021+614		QSS		+61 27 18.1	2.2	2.3	3.0	L,C,U
2029+121		QSS	20 29 32.68	+12 09 28.8	1.0	1.0 0.6		L,C
2037-253		QSS	20 37 10.77	-25 18 26.4	0.9			
2106-413		222	21 06 19.40	-41 22 33.4	1.3	2.2		
2113+293		QSS	21 13 20.58	+29 21 06.5	0.9	0.8		т С
2128+048			21 28 02.62	+04 49 04.2	4.1	2.1	4 6	L,C
2128-123		QSS	21 28 52.68	-12 20 20.6	1.4	2.4	4.6	L,C
2131-021	4C-02.81	QSS	21 31 35.19	-02 06 40.0 +00 28 25.2	1.9	1.9	6.9	L,C,U
2134+004		QSS	21 34 05.19		3.6	10.3		

TABLE III. (continued)

Source	Other Name	Optical ID	^α (1950)	^δ (1950)	s ₂₀	s ₆	s_2	VLA
2144+092*	***	QSS	21 44 42.48	+09 15 51.4	0.9	0.7	-	
2145+067	4C+06.69	QSS	21 45 36.08	+06 43 40.9	1.1	2.5		
2149-307			21 49 00.60	-30 42 00.2	1.1	1.1		
2149+056		QSS	21 49 07.71	+05 38 06.8	0.9	1.0		
2150+173		GAL	21 50 02.24	+17 20 29.8	0.8	0.7		L,C
2200+420		QSS	22 00 39.36	+42 02 08.57	2.2	2.4	2.5	L,C,U
2203-188*	*	QSS	22 03 25.72	-18 50 17.0	6.2	4.1	2.3	L,C
2210+016	4C+01.69		22 10 05.12	+01 37 59.4	2.5	1.0		
2210-257*	***	QSS	22 10 14.14	-25 44 22.5	1.0	0.9		
2216-038	4C-03.79	QSS	22 16 16.39	-03 50 40.7	0.7	3.2		
2227-088		QSS	22 27 02.33	-08 48 17.5	1.4	1.2		
2227-399*	***	QSS	22 27 45.01	-39 58 16.7	0.6	0.6		
2230+114	4C+11.69	ល្អនន	22 30 07.812	+11 28 22.7	6.2	3.6	3.7	L
2234+282		QSS	22 34 01.74	+28 13 23.2	1.1	1.3		L,C
2240-260		QSS	22 40 41.82	-26 00 14.8	0.7	0.6		,
2243-123		QSS	22 43 39.80	-12 22 40.2	2.3	2.4		
2245-328		QSS	22 45 51.44	-32 51 42.5	1.6	1.8	2.6	С
2247+140*	4C+14.82	QSS	22 47 56.71	+14 03 57.4	1.9	1.1		L
2254+074		QSS	22 54 45.99	+07 27 08.9	0.4	0.5		С
2255-282		QSS	22 55 22.36	-28 14 27.4	1.1	1.6		
2318+049		QSS	23 18 12.13	+04 57 23.4	0.4	0.8		
2319+272**	***4C+27.50	QSS	23 19 31.98	+27 16 19.1	1.1	0.8		
2328+107	4C+10.73	QSS	23 28 08.77	+10 43 45.5	1.0	1.1		
2329-162		QSS	23 29 02.40	-16 13 30.9	1.1	0.9		
2331-240		GAL	23 31 17.98	-24 00 17.0	1.0	1.0		С
2337-334			23 37 16.63	-33 26 56.4	1.2	0.8		-
2337+264		QSS	23 37 58.29	+26 25 18.9	0.9	0.8		С
2344+092**	**4C+09.74	QSS	23 44 03.78	+09 14 05.4	1.7	1.9		-
2345-167*		QSS	23 45 27.691	-16 47 52.6	3.4	2.7	3.1	С
2351+456	4C+45.51	GAL	23 51 49.97	+45 36 22.7	2.1	1.2		-
2352+495		GAL	23 52 37.790	+49 33 26.79	2.4	1.7	0.8	L,C,U

a Sources marked with asterisks have been observed in very recent VLA calibration runs with some degree of resolution being found, as specified below. Such observations and refinements are constantly being made during the calibration program.

while multicomponent sources have positions listed for each of the radio peaks that we consider significant. Column 6 gives the total and peak flux densities at 4900 MHz (λ 6 cm) for each source, with the flux density always referring to the dominant component. Column 7 gives total and peak flux densities at 1480 MHz (λ 20 cm). Here, the top line refers to the total emission from

the entire source and the peak flux density of the dominant component. Subsequent lines, when present, give peak flux densities for the additional components whose positions are listed in columns 4 and 5. We note that our 4900-MHz measurements underestimate the total flux density for a number of well resolved sources owing to the lack of short spacings mentioned above; previous

^{*} core-hole resolved at 3 km

^{**} resolved at spacings > 10 km

^{***} Heavily resolved double

^{****} core-hole resolved at 6 km

^{*****} slightly resolved at spacings > 10 km

TABLE IV. Resolved sources.

		Other	Optical	Positi		6 cm Total Flux	20 cm Total Flux	Comments
Sourc	e	Name	I.D.	α(1950)	^δ (1950)	Peak Flux	Peak Flux	
0003-003		3C2	QSS	00 ^h 03 ^m 48.85	-00°21'06"	1.5/0.6	3.8/2.0	Complex source may contain three components
0010+405	A D	4C+40.01	GAL	00 10 54.26 00 10 55.50	+40 34 57 +40 34 52	0.7/0.5	1.6/0.5 0.1/0.1	Complex source structure with two dominant components.
0021-297			QSS			0.9/0.1	1.7/0.4	20 cm size ∿ 20"
0034-014	A B	3C15	GAL	00 34 30.38 00 34 31.08	-01 25 35 -01 25 54	0.5/0.1	3.2/0.6 /0.3	Two dominant components.
0035-024	A B	3C17	GAL	00 35 46.97 00 35 47.37	-02 24 05 -02 24 13	2.0/0.5	5.2 0.6 /0.5	Two componentscomponent B resolved.
0038+097	A B C	3C18	GAL	00 38 14.48 00 38 12.72 00 38 13.80	+09 46 53 +09 47 22 +09 46 38	0.8/0.1	3.1/0.2 /0.2 /0.1	Three major components with extended emission.
0039-445			GAL				3.0/2.0	Double; Ratio 2:1, 9" separation, visibilities only.
0055-016		3C29	GAL '	00 55 02.00	-01 38 56	0.3/0.1	3.8/0.2	Extended emission; flux uncertain.
0055+300			GAL				1.0/0.4	Visibilitiessize ∿ 3".5
0113-118			QSS	01 13 41.8	-11 51 50	1.2/	1.2/	400 mJy in halo at 20 cm. Position based on only one scan.
0114-211			GAL	01 14 25.95	- 21 07 57	1.1/0.9	3.7/2.8	Resolved Gaussian size \sim 2" at 6 cm.
0116+082		4C+08.06	GAL	01 16 24.24	+08 14 10	1.1/0.9	2.5/1.7	Extended along beam?
0118-272			QSS	01 18 09.67	-27 17 11	0.9/0.8	1.1/0.8	Resolved at 6 cm. Gaussian size \sim 2".
0122-003			QSS	01 22 55.11	-00 21 30	1.4/1.2	1.4/0.9	Slightly resolved. Three components. Direction along p.a90° and 140° from dominant source.
0127+233		3C43	QSS	01 27 14.96	+23 22 53	1.1/0.8	3.0/1.9	Slightly resolved.
0159-117		3C57	QSS				2.8/1.5	Visibilityone scan.
0218+357			GAL	02 18 04.16	+35 42 32	1.2/0.6	1.7/1.0	Extended emission along p.a55°.
0235-197	A B C D		GAL	02 35 25.90 02 35 24.78 02 35 24.21 02 35 23.27	-19 45 32 -19 45 17 -19 45 23 -19 46 11	1.0/0.1	3.5/0.9 /0.4 /0.3 /0.6	Four major components. Possible emission 70" N.W.
0240-002	A B C	3C71	GAL	02 40 07.01 02 40 07.19 02 40 06.93	-00 13 30 -00 13 28 -00 13 36	1.8/0.1	4.3/1.3 /1.1 /0.2	
0347+057	A B	4C+05.16		03 47 07.40 03 47 06.66	+05 42 11 +05 43 15	1.0/0.3	2.8/1.3 /0.5	Wide double?
0402+379		4C+37.11	GAL	04 02 29.88	+37 55 27	1.1/0.9	1.7/1.2	Slightly resolved along p.a. 5° and -110° .
0453-206	A B C		GAL	04 53 13.94 04 53 16.49 04 53 15.42	-20 38 55 -20 38 52 -20 41 28	1.5/0.1	4.4/1.4 /0.5 /0.2	Components A & B resolved. Peak flux refer to map with 3 km taper.
0453-301			GAL			0.4/0.0	3.3/0.1	Heavily resolved \sim 15" Gaussian size.
0518+165		3C138	QSS	05 18 16.56	+16 35 26	4.1/1.6	8.6/7.7	Slightly extended in p.a. 90°.

TABLE IV. (continued)

				Positio		6 cm	20 cm	
Sourc	е	Other Name	Optical I.D.	α(1950)	δ (1950)	Total Flux Peak Flux	Total Flux Peak Flux	Comments
)521-365			GAL			3.2/1.7	16.5/2.0	Gaussian size ∿ 12" at 20 cm.
0539-057	А		QSS	05 30 10.99	-05°43'15"	1.5/1.4	1.3/0.7	A resolved.
	В		2	05 39 12.24	-05 42 52	,	/0.2	
	C D			05 39 13.11 05 39 12.07	-05 43 17 -05 43 00		/0.1 /0.1	
0602-319			QSS	06 02 22.45	-31 55 40	1.1/0.1	2.9/1.5	Resolved Gaussian size \sim 3.5.
0604-203			GAL			0.4/0.1	3.1/0.5	Gaussian size \sim 7" at 20 cm.
0614-349			GAL	06 14 48.80	-34 55 12.2	1.3/0.9	2.8/2.7	Resolved Gaussian size \sim 2" at 6 cm.
0624-058	A B	3C161	GAL	06 24 43.21 06 24 44.41	-05 51 12 -05 50 46	6.6/2.4	17.6/8.0 /1.4	A is double of separation 3" along p.a8 ratio 3:1, some extended structure.
0646-306				06 46 19.22	-30 40 55	0.7/0.7	1.0/0.7	Resolved.
0704-231				07 04 27.22	-23 06 55	1.5/1.0	3.6/1.9	Resolved.
0715-250	A B			07 15 13.10 07 15 14.13	-24 59 21 -24 59 41	1.2/0.2	4.1/1.7 /0.6	Both components resolved.
0723+679		3C179	Qss	07 23 05.71	+67 54 54	0.8/0.4	2.2/0.6	Component A resolved along p.a. 90°.
	B C			07 23 04.21 07 23 03.29	+67 54 53 +67 54 52		/0.4 /0.4	Component C resolved along p.a. 170°.
0741-063		4C-06.18		07 41 54.69	-06 22 20	3.0/2.6	8.0/6.4	Slightly resolved.
0745+241			QSS	07 45 35.71	+24 07 46	1.2/0.9	0.8/0.5	Slightly resolved in p.a. \sim 90°.
0755+379		3C189	GAL	07 55 08.97	+37 55 22	0.3/0.2	2.2/0.2	Complex source. Many components.
0805-077	A		QSS	08 ^h 05 ^m 50. ^s 56	-07°42'22"	1.0/0.9	1.3/1.0	Two components.
	В			08 05 49.60	-07 42 37		/0.2	
0812+367			QSS	08 12 10.73	+36 44 27	0.9/0.8	0.9/0.7	May be close double in p.a. \sim -20°.
0820+225		4C+22.21	QSS	08 20 28.49	+22 32 45	1.8/1.5	2.2/1.8	Slightly resolved?
0825-202			QSS	08 25 01.49	-20 16 47	1.1/0.5	3.7/1.9	Double with probable background source.
	B C			08 25 02.32 08 25 04.22	-20 16 59 -20 16 58		/0.9 /0.4	
0850+581	Δ	4C+58.17	QSS	08 50 50.24	+58 08 56	0.8/0.2	1.3/0.6	A resolved in p.a. ∿ 90°. B has weaker
00501501	В	40.30.17	255	08 50 49.49	+58 08 58	0.0/0.2	/0.1	counterpart on other side of A. C is back
	С			08 50 46.79	+58 08 45		/0.1	ground sourcemay not be completely real.
0858-279			QSS	08 48 31.51	- 27 56 33	1.7/1.6	2.4/1.8	Resolved.
0859-257			QSS	08 59 37.74	-25 43 39	1.2/0.1	5.3/1.6	Triple source. Component C resolved in
	B C			08 59 35.15 08 59 36.71	-24 43 13 -25 43 24		/1.3 /0.4	p.a. ∿ 30°. Other components slightly resolved.
0859+470	-		QSS	08 59 40.01	+47 02 57	1.6/1.4	2.3/1.9	Gaussian size \sim 6" at 6 cm.
0906+430		3C216	QSS	09 06 17.29	+43 05 59	1.8/1.0	4.2/3.1	Slightly resolved in p.a. ~ 30°.
0920-397	А		2					
0920-39/	A B			09 20 48.23 09 20 48.23	-39 46 41 -39 46 48	1.9/1.5	2.6/1.3 /0.2	Triple source.
	С			09 20 48.17	-39 46 34		/0.1	
0945+664		4C+66.09)	09 45 14.88	+66 28 58	1.2/0.8	2.3/1.9	Slight resolution, p.a. ∿ 25°.

TABLE IV. (continued)

				Posit	ion	6 cm	20 cm	
Sourc	e	Other Name	Optical I.D.	α(1950)	δ (1950)	Total Flux Peak Flux	Total Flux Peak Flux	Comments
0949+002	A B	3C230	QSS	09 49 25.10 09 49 24.89	+00 12 38 +00 12 44		3.0/1.4 /1.2	Clear double.
0954+556		4C+55.17	QSS	09 54 14.36	+55 37 16	2.1/1.8	3.2/2.6	May be slight extension in p.a. \sim -60°.
1005+077	A B	3C237		10 05 21.99 10 05 24.57	+07 44 59 +07 45 26	2.1/1.0	5.9/4.7 /0.6	Main component seems unresolved. Secondary background source?
1018-426	A B C			10 17 56.18 10 17 56.77 10 17 58.65	-42 36 28 -42 36 16 -42 36 17	1.1/0.1	4.1/2.3 /0.4 /0.3	Component A slightly extended in p.a. \sim 175°?
1030+415			QSS				0.8/0.6	Visibilities only.
1039+029	A B	4C+03.18	GAL	10 39 04.03 10 39 04.25	+02 58 12 +02 58 16	1.0/0.3	2.9/0.8 /0.8	Doubleboth components look unresolved. Many 10-15% background sources in map.
1045-188			QSS	10 45 40.11	-18 53 44	0.7/0.6	1.1/0.4	Slightly extended in most directions.
1046-409	A B			10 46 22.68 10 46 22.39	-40 58 07 -40 58 00	0.9/0.4	2.1/0.5 /0.5	Small halo in p.a. \sim 160°. Lots of sidelobes.
1049+215		4C+21.28	Qss	10 49 07.16	+21 35 49	1.2/1.0	1.1/0.9	Gaussian size \sim 7" at 20 cm.
1055+201	A B	4C+20.24	QSS	10 55 37.10 10 55 37.56	+20 08 16 +20 07 55	1.5/0.4	2.0/1.2 /0.3	Component A slightly resolved.
1104-445			QSS			0.0/0.0	0.7/0.1	Gaussian size \sim 6" at 20 cm.
1150+497	A B C	4C+49.22	QSS	11 50 48.00 11 50 47.93 11 50 48.07	+49 47 50 +49 47 46 +49 47 58	0.9/0.6	1.6/0.6 /0.2 /0.1	Complex triple source with halo.
1203+645		3C268.3	GAL	12 03 54.08	+64 30 19	1.2/0.8	3.8/3.0	Structure 1-2" S.E. of peak. Very close double or point source?
1210+134		4C+13.46	QSS	12 10 59.21	+13 24 02	0.8/0.8	1.4/1.1	Slightly resolved.
1213-172				12 13 11.72	-17 15 04	1.9/1.5	1.6/1.2	Slightly resolved.
1221-423	A B		GAL	12 21 02.57 12 21 05.27	-42 18 52 -42 18 47	1.0/0.3	2.3/1.8 /0.3	Component A probably somewhat resolved.
1222+216	A B C	4C+21.35	QSS	12 22 23.44 12 22 24.16 12 22 23.30	+21 39 23 +21 39 25 +21 39 15	1.2/0.8	1.7/0.7 /0.3 /0.1	Component B resolved in N.W. at p.a. \sim -20° \rightarrow -50°.
1222+131		3C272.1	GAL	12 22 31.5	+13 09 46	0.6/0.2	4.0/0.4	Highly resolved. Peak refers to 1 km taper map.
1226+023	A B	3C273	QSS	12 26 33.24 12 26 32.93	+02 19 44 +02 19 39	38.8/33.0	45.8/26.5 /9.1	Double.
1244-255			QSS	12 44 06.70	-25 31 26	1.6/1.4	1.2/1.0	Possible resolution.
1249+092	A B C D		GAL	12 49 13.18 12 49 12.24 12 49 09.82 12 49 08.53	+09 12 45 +09 12 36 +09 12 29 +09 12 12	0.3/0.0	1.7/0.4 /0.1 /0.1 /0.4	Double radio source with four main components. Bad sidelobes.
1251+159		4C+15.40	GAL	12 51 02.89	+15 58 41	0.6/0.1	1.7/0.8	Resolved in p.a. ∿ 70°. May be close double.

TABLE IV. (continued)

				Positi		6 cm	20 cm	
Source	9	Other Name	Optical I.D.	α(1950)	^δ (1950)	Total Flux Peak Flux	Total Flux Peak Flux	Comments
1253-055	A B C	3C279	QSS	12 53 35.13 12 53 35.04 12 53 34.87	-05 31 18 -05 31 19 -05 31 11	11.7/10.5	11.0/6.2 /0.8 /1.8	Probably has three close components.
1317+179	A B	4C+17.56		13 17 55.16 13 17 54.47	+17 58 57 +17 58 51	0.6/0.1	1.7/0.6 /0.2	Component A slightly resolved. Component B clearly resolved in p.a. \sim -170°.
1414-037		3C297		14 14 47.58	-03 46 56	0.7/0.4	2.4/1.3	Resolved.
1424-418			QSS	14 24 46.71	-41 52 56	2.1/1.8	3.7/2.1	Extension basically along beam in p.a. \sim -10
1434+036		4C+03.30	GAL	14 34 25.85	+03 37 10	1.2/0.4	2.8/1.0	Resolved in p.a100° and p.a. 140°. Severa sources aliased in from outside map.
1508-055		4C-05.64	QSS	15 08 14.94	-05 31 49	2.1/0.8	3.8/1.9	Resolved.
1509+015	A B			15 09 53.00 15 09 52.87	+01 32 25 +01 32 19	0.8/0.2	2.2/0.8 /0.5	Two dominant components. Component B resolved in p.a70°.
1538+149		4C+14.60	QSS	15 38 30.50	+14 57 24	1.5/1.2	1.7/1.2	Slightly resolved.
1548+056		4C+05.64	QSS	15 48 06.87	+05 36 13	2.1/1.8	2.3/2.1	Slightly resolved along p.a. 130°.
1550-269				15 50 59.64	- 26 55 50	1.5/1.2	1.4/1.0	May be slightly resolved.
1557+708		4C+70.19	GAL			0.1/0.0	0.7/0.1	Heavily resolved. Visibilities only.
1602+014	A B	3C327.1	GAL	16 02 12.54 16 02 13.23	+01 26 01 +01 25 57	1.1/0.1	4.3/1.1 /1.1	
1603+001		4C+00.58	GAL	16 03 39.35	+00 08 34	0.9/0.1	2.2/0.3	Unequal double.
1606+106		4C+10.45	QSS	16 06 23.40	+10 37 00	1.6/1.5	1.2/0.5	Complex area. Several sources.
1622-253	A B			16 22 44.02 16 22 44.26	-25 20 51 -25 20 55	3.4/3.1	1.9/1.0 /0.2	Two components. Complex area.
1629+120		4C+12.59	QSS	16 29 24.59	+12 02 24	0.8/0.5	1.6/1.2	Resolved along p.a90° and -15°.
1655+077			QSS	16 55 43.95	+07 46 00	1.8/1.5	1.6/1.0	Resolved.
1656+053	A		QSS	16 56 05.62	+05 19 47	2.1/1.8	1.7/1.2	Resolved.
1800+440			QSS	18 00 03.20	+44 04 18	0.9/0.7	0.9/0.5	Probable double, resolved along p.a150°.
1821-327				18 21 41.17	-32 44 39	0.6/0.1	4.0/0.5	Very complex area.
1823+568		4C+56.27	Qss	18 23 14.94	+56 49 18	1.6/1.3	1.5/0.9	Resolved along p.a. 80°.
1827-360				18 27 36.87	-36 04 38	1.3/	7.0/6.8	Equal double at 6 cm $^{\circ}$ 1" separation.
1828+487		3C380	QSS	18 28 13.47	+48 42 41	6.0/2.4	14.6/7.0	Resolved along p.a60° and +140°.
1829+290		4C+29.56		18 29 17.94	+29 04 58	1.5/1.1	3.7/2.7	Resolved along p.a50°.
1830+285	A B C	4C+28.45	QSS	18 30 51.59 18 30 52.35 18 30 52.79	+28 31 27 +28 31 17 +28 31 05	1.2/0.6	1.7/0.4 /0.2 /0.2	Triple source with halo.
1859-235,	A B			18 59 47.40 18 59 43.18	-23 34 18 -23 33 44	1.1/0.6	2.9/1.8 /0.4	Unequal double
1938-155	A B C		GAL	19 38 24.32 19 38 25.99 19 38 24.86	-15 31 31 -15 31 42 -15 31 32	2.2/0.5	5.8/2.7 /1.4 /0.5	Component A resolved along p.a47° (the beam!)

TABLE IV. (continued)

				Posit		6 cm	20 cm	
Sour	ce	Other Name	Optical I.D.	α(1950)	^δ (1950)	Total Flux Peak Flux	Total Flux Peak Flux	Comments
1939+605	A	3C401	GAL	19 39 ^m 38.51	+60°34'27"	1.2/0.1	4.0/0.6	Components A, B, C, extended structure.
	В			19 39 39.22	+60 34 40		/0.4	
	С			19 39 38.25	+60 34 25		/0.4	
1954+513			Qss	19 54 22.48	+51 23 46	1.4/1.1	1.9/1.4	Resolved.
2012+234	Α	3C409		20 12 18.47	+23 25 33	3.3/0.3	12.0/3.1	Triple source. All resolved.
	В			20 12 17.72	+23 25 50		/3.0	
	С			20 12 18.28	+23 25 57		/0.7	·
2126-158				21 26 26.90	-15 51 54			Resolved 15%. Size \sim 8" VLA calibration run
2135-209				21 35 01.39	-20 56 05	1.4/1.1	3.9/2.6	Resolved?
2149-287				21 49 10.65	-28 42 26	1.2/0.5	2.8/1.6	Gaussian size \sim 2" at 6 cm.
2201+315	A	4C+31.63	QSS	22 01 00.84	+31 31 06	2.2/1.7	2.2/1.0	Component A slightly resolved.
	В			22 01 01.76	+31 31 07		/0.2	
2209+080	А	4C+08.64	oss	22 09 32.14	+08 04 27	0.8/0.3	1.3/0.7	Component A resolved in p.a. ∿ 180°.
	В		-	22 09 32.80	+08 04 33		/0.2	•
2226-411			QSS	22 26 22.22	-41 06 54	1.0/0.5	2.7/1.5	Gaussian size \sim 4" at 6 cm.
2314+038	А	3C459	GAL	23 14 02.37	+03 48 55	1.4/0.4	3.7/2.9	Component A slightly resolved in p.a.
	В			23 14 01.85	+03 48 56		/0.4	√ 100°?
2323+435			GAL	23 23 18.29	+43 30 28		3.0/0.1	Heavily resolved.
2323-407			GAL	23 23 51.69	-40 43 48	1.0/0.4	3.0/2.0	Resolved.
2324+405	A	3C462	GAL	23 24 31.04	+40 31 46	0.8/0.1	2.3/0.4	Component A is resolved along p.a. 45°, and
	В			23 24 29.74	+40 31 29		/0.4	is probably double. Component B is also well resolved, and extended in p.a. $\sim 100^{\circ}$.

single-dish measurements are probably more accurate than our VLA values in such cases. In column 8, we comment on the source structures. The Gaussian sizes referred to are FWHM.

Samples of the source maps are displayed in Figs. 1(a)-1(v). Most of the sources shown in these maps lie near or below the celestial equator and have not had high-resolution maps previously displayed in the literature. The full width half-power synthesized beam is shown as a cross-hatched ellipse. Significant sidelobes remain in many maps because of our intermittent sampling of the u-v plane, so the reality of features containing less than about 5%-10% of the peak flux density is questionable.

III. COMPLETE SAMPLE OF STRONG 5-GHz RADIO SOURCES

In order to provide a complete flux density sample for a statistical study, we require a more careful selection of sources than is possible from our observations alone. Therefore we have constructed a sample of strong extragalactic radio sources from those observed in the Parkes and S surveys.

a) Construction of the Complete Sample

Our sample is intended to include all extragalactic radio sources having $70^{\circ} \gtrsim \delta \gtrsim -45^{\circ}$, $|b| \gtrsim 10^{\circ}$, and 5-GHz flux densities greater than 1 Jy in the Parkes and S surveys. Because of source variability, some of the sources in the original surveys will be less than 1 Jy. Other sources may now have flux densities greater than 1 Jy.

The single-dish surveys from which we draw our sample contain a total of 454 objects meeting the flux density criterion specified above. Ten of these objects are known or suspected to be galactic in origin. Removing these sources, which are listed in Table V, leaves us with a total of 444 extragalactic radio sources. This complete sample contains 157 galaxies, 230 quasars, and 57 sources with no known optical counterparts.

A total of 291 of the members of our complete sample have been observed by us at the VLA. The remaining 153 sources were not studied in our observations because they contained previously well determined structure or because we were unable to fit them into our observing schedule. Information on these sources was

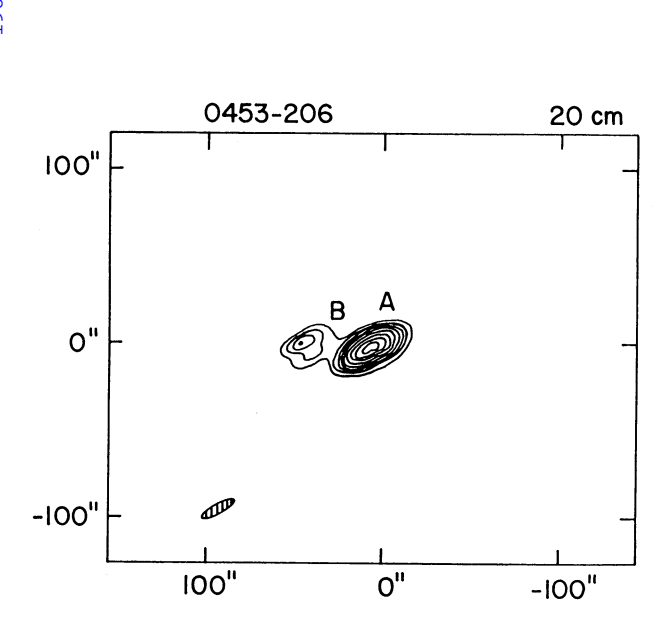


FIG. 1(a). For this and all subsequent maps of Fig. 1, the wavelength is $20\,\mathrm{cm}$ (1480 MHz), and the contour levels are -5%, 5%, 10%, 15%, 20%, 25%, 35%, 50%, 65%, and 85% of the peak flux. Negative contours are denoted by dashed lines. Right ascension and declination are given as offsets in arcseconds from the (0'', 0'') position, whose 1950.0 coordinates are given for each map. Gaussian tapers were applied to the observed correlated visibilities with the half-power spacing of the taper specified separately for each map. This map of the source 0453-206 was made with a 3-km taper, has a peak flux of 1.38 Jy, and has coordinates offset from $\alpha=04^{\rm h}53^{\rm m}13^{\rm s}29$, $\delta=-20^{\rm o}38'52''0$.

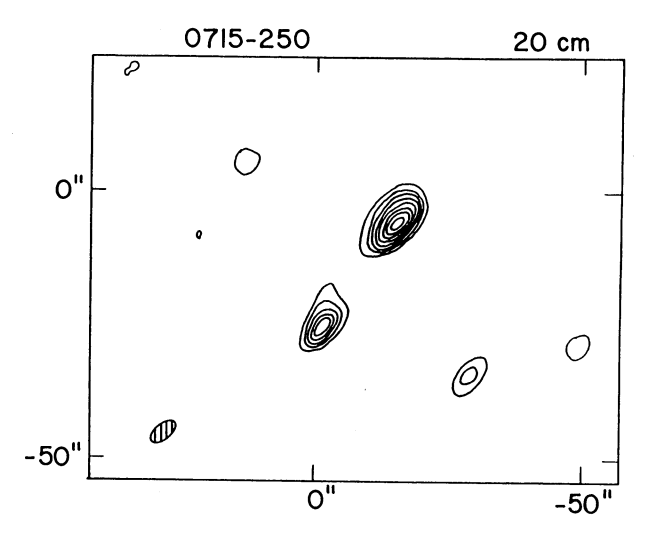


FIG. 1(b). Source: 0715 - 250; taper: 10 km; peak flux: 1.64 Jy; offsets from $\alpha=07^{\rm h}15^{\rm m}14{\rm s}19$, $\delta=-24^{\circ}59'58''$.

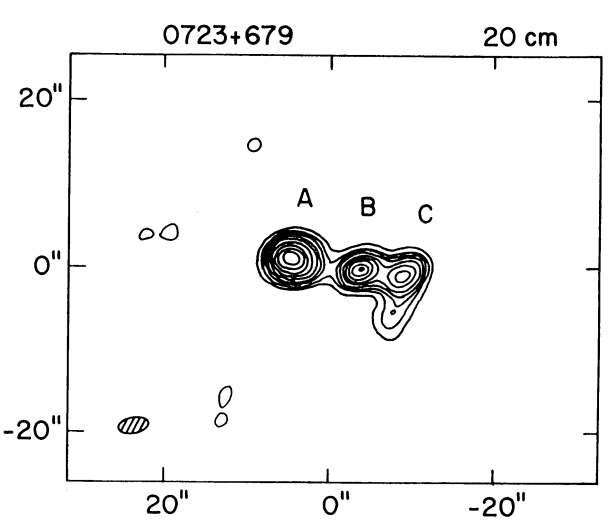


FIG. 1(c). Source: 0723 + 679; taper: 15 km; peak flux: 0.55 Jy; offsets from $\alpha = 07^{\rm h}23^{\rm m}0489$, $\delta = +67^{\rm e}54'53''.0$.

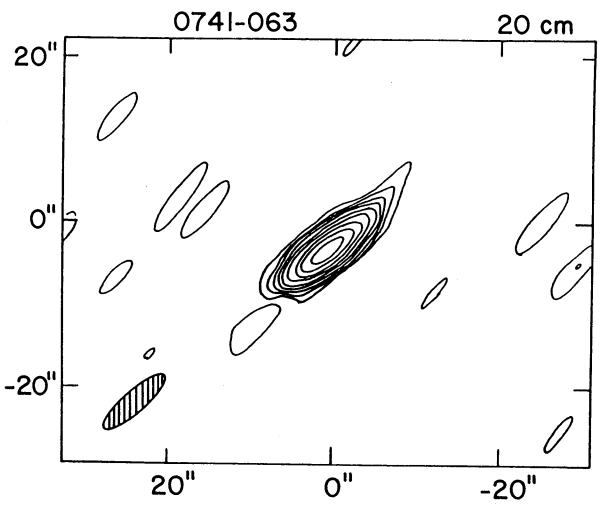


FIG. 1(d). Source: 0741 - 063; taper: 15 km; peak flux: 6.36 Jy; offsets from $\alpha = 07^{\rm h}41^{\rm m}54!59$, $\delta = -06^{\circ}22'16''.0$.

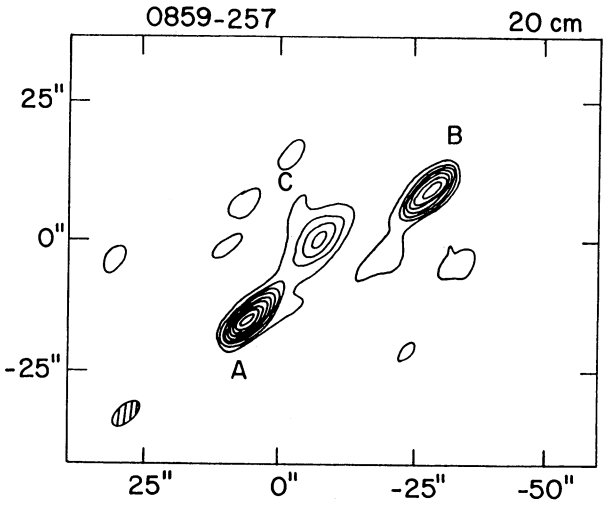
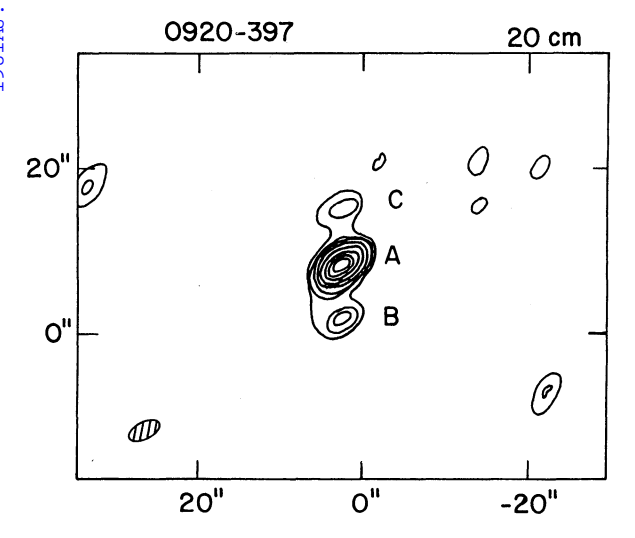


Fig. 1(e). Source: 0859 - 257; taper: 10 km; peak flux: 1.59 Jy; offsets from $\alpha = 08^{h}59^{m}37529$, $\delta = -25^{\circ}43'24''0$.



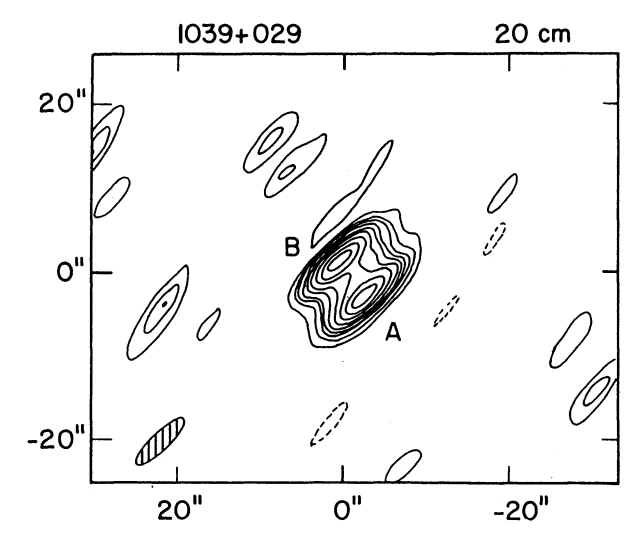
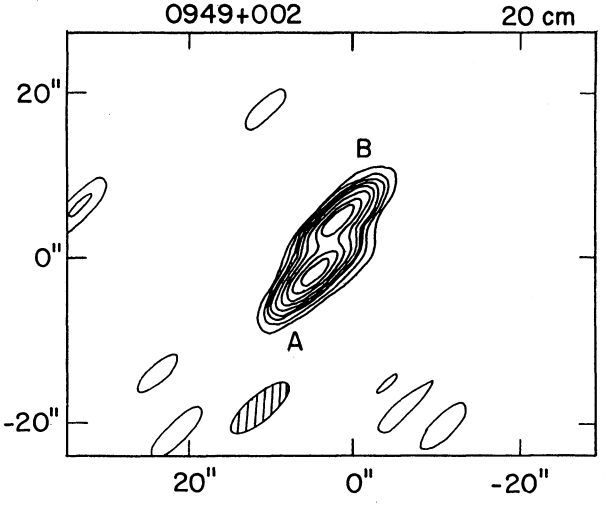


Fig. 1(f). Source: 0920 – .397; taper: 15 km; peak flux: 1.26 Jy; offsets from $\alpha = 09^{\rm h}20^{\rm m}47{\rm s}99$, $\delta = -39^{\rm s}46'50{\rm s}0$.

Fig. 1(i). Source: 1039 + 029; taper: 15 km; peak flux: 0.75 Jy; offsets from $\alpha = 10^{h}39^{m}04$?19, $\delta = + 02^{\circ}58'15''0$.



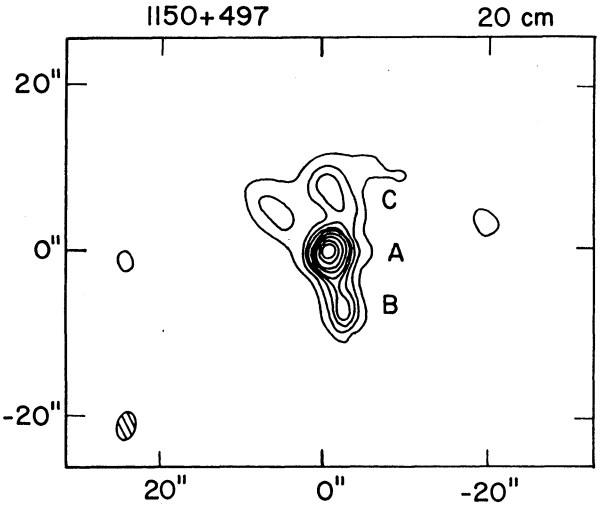
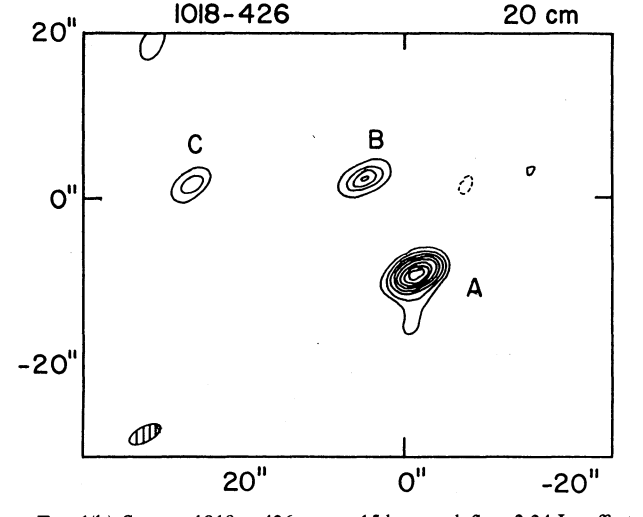


Fig. 1(g). Source: 0949 + 002; taper: 15 km; peak flux: 1.43 Jy; offsets from $\alpha=09^{\rm h}49^{\rm m}24.79$, $\delta=+00^{\rm o}12'39.0$.

Fig. 1(j). Source: 1150+ 497; taper: 15 km; peak flux: 0.57 Jy; offsets from $\alpha=11^{\rm h}50^{\rm m}48^{\rm s}06$, $\delta=+49^{\rm s}47'50''0$.



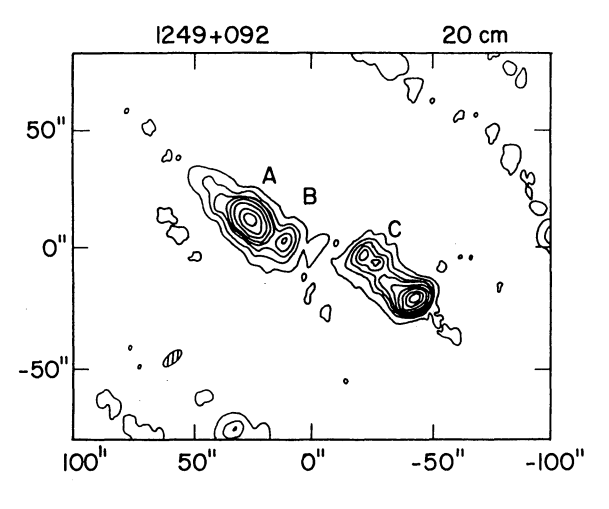


Fig. 1(h). Source: 1018-426; taper: 15 km; peak flux: 2.24 Jy; offsets from $\alpha=10^{\rm h}17^{\rm m}56$;29, $\delta=-42^{\rm s}36$;19."0.

Fig. 1(k). Source: 1249 + 092; taper: 5 km; peak flux: 0.27 Jy; offsets from $\alpha = 12^{\rm h}49^{\rm m}11^{\rm s}49$, $\delta = +09^{\rm s}12'34''.0$.

© American Astronomical Society • Provided by the NASA Astrophysics Data System

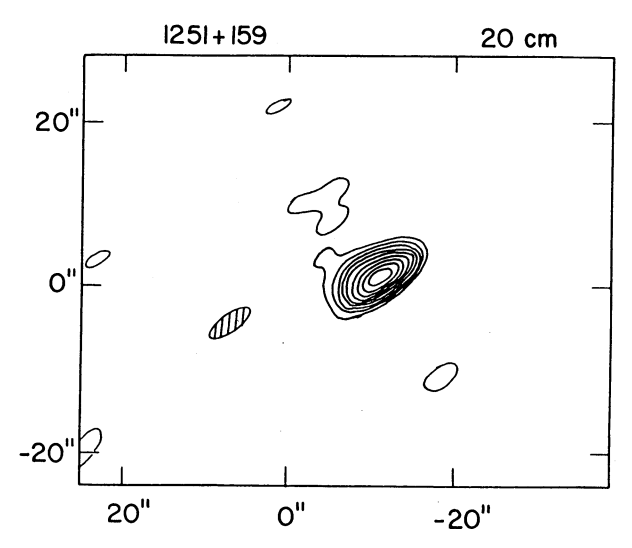
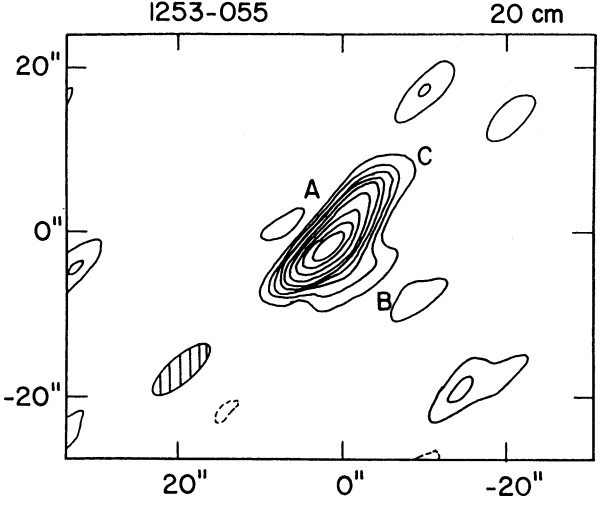


Fig. 1(1). Source: 1251 + 159; taper: 15 km; peak flux: 0.78 Jy; offsets from $\alpha = 12^{\rm h}51^{\rm m}03^{\rm s}68$, $\delta = +15^{\rm s}58'40''0$.

Fig. 1(o). Source: 1508 - 055; taper: 15 km; peak flux: 2.26 Jy; offsets from $\alpha=15^{\rm h}08^{\rm m}15^{\rm h}03$, $\delta=-05^{\rm s}31'46''0$.



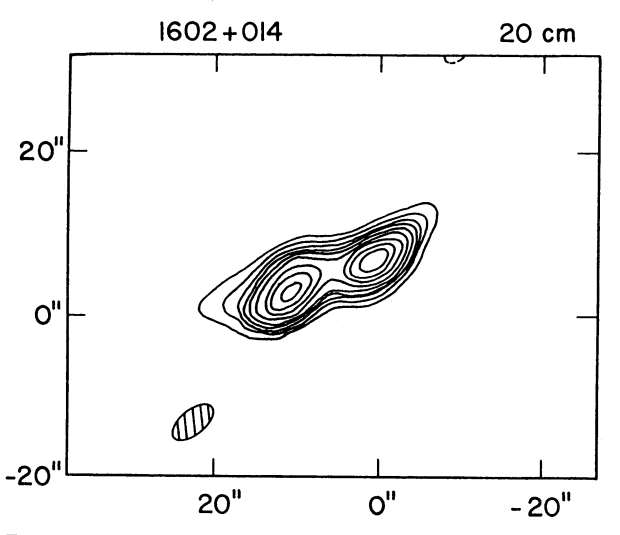
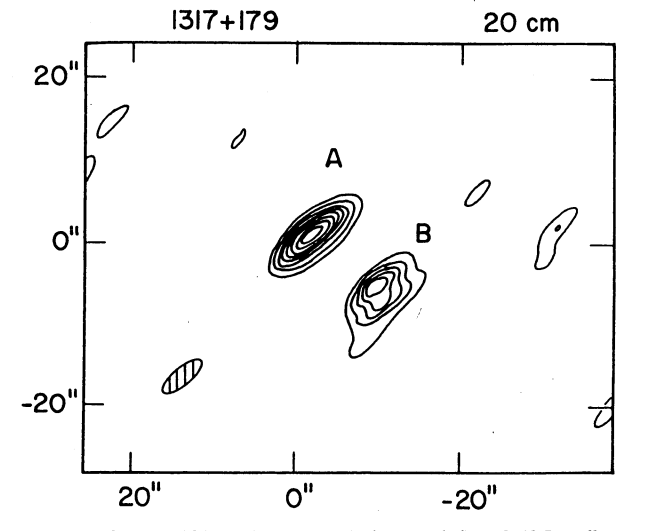


Fig. 1(m). Source: 1253 — 055; taper: 15 km; peak flux: 6.15 Jy; offsets from $\alpha=12^{\rm h}53^{\rm m}35!83$, $\delta=-05^{\rm s}31'08"0$.

Fig. 1(p). Source: 1602+ 014; taper: 15 km; peak flux: 1.06 Jy; offsets from $\alpha=16^{\rm h}02^{\rm m}12^{\rm s}49,\,\delta=+01^{\rm s}25'54\rlap.{''}0.$



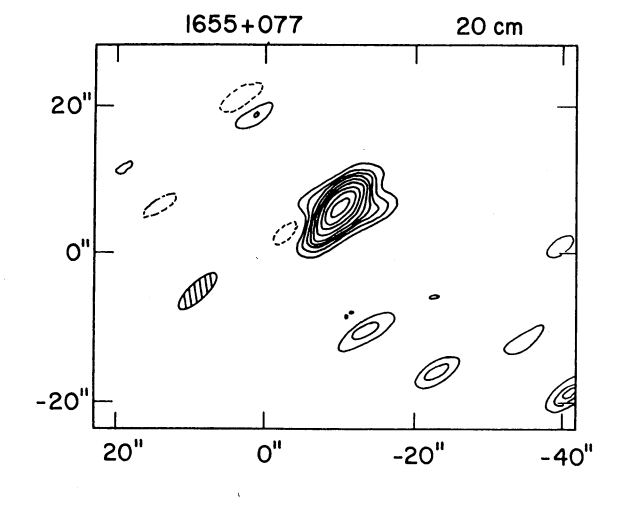


Fig. 1(n). Source: 1317 + 179; taper: 15 km; peak flux: 0.60 Jy; offsets from $\alpha=13^{\rm h}17^{\rm m}55^{\rm s}28$, $\delta=+17^{\rm s}58'56''$ 0.

Fig. 1(q). Source: 1655 + 077; taper: 15 km; peak flux: 0.95 Jy; offsets from $\alpha = 16^{\rm h}55^{\rm m}44^{\rm s}59$, $\delta = +07^{\rm o}45'55''$ 0.

© American Astronomical Society • Provided by the NASA Astrophysics Data System

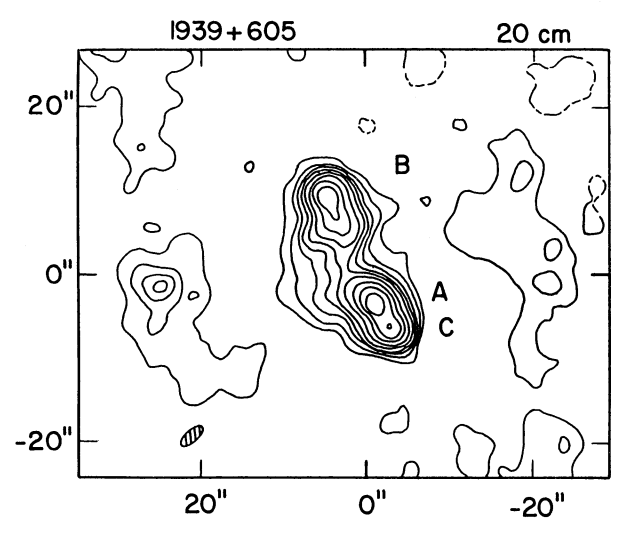


Fig. 1(r). Source: 1939 + 605; taper: 15 km; peak flux: 0.55 Jy; offsets from $\alpha = 19^{\rm h}39^{\rm m}38^{\rm s}57$, $\delta = +60^{\circ}34'30''.0$.

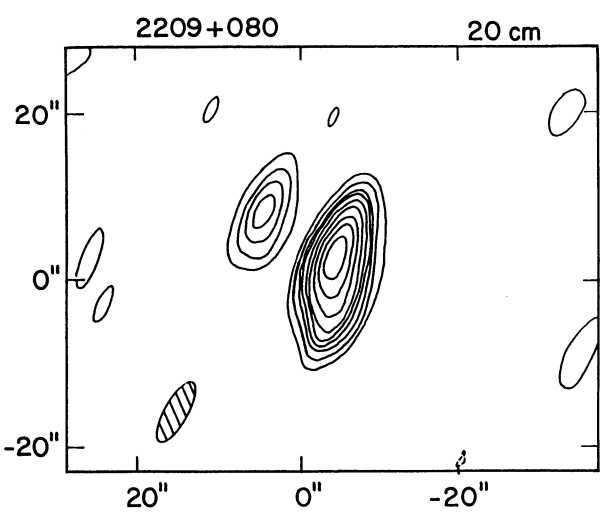


FIG. 1(t). Source: 2209 + 080; taper: 15 km; peak flux: 0.69 Jy; offsets from $\alpha = 22^{\text{h}}09^{\text{m}}32^{\text{s}}39$, $\delta = +08^{\circ}04'25''0$.

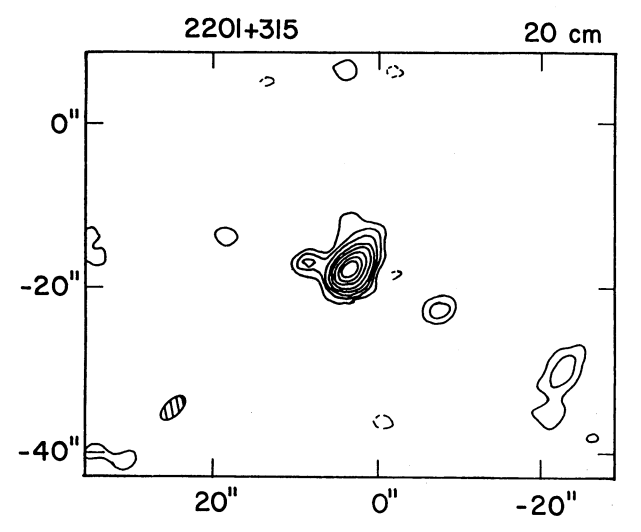


Fig. 1(s). Source: 2201 + 315; taper: 15 km; peak flux: 0.96 Jy; offsets from $\alpha = 22^{\rm h}01^{\rm m}01^{\rm s}08$, $\delta = +31^{\circ}31'24''0$.

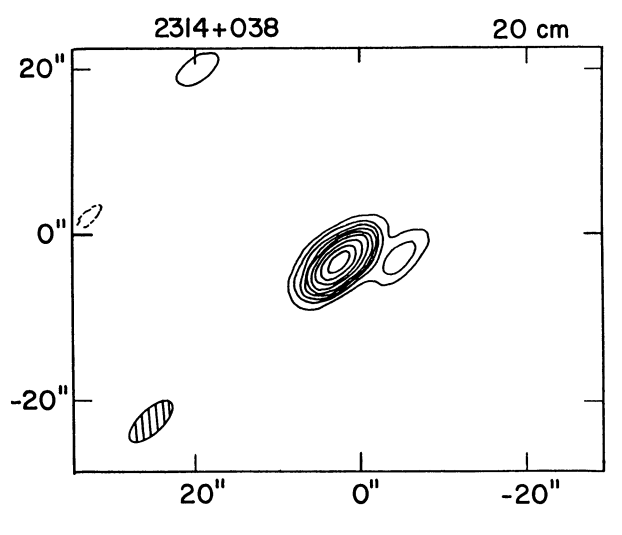


Fig. 1(u). Source: 2314+ 038; taper: 15 km; peak flux: 2.92 Jy; offsets from $\alpha=23^{\rm h}14^{\rm m}02^{\rm s}19,\,\delta=+03^{\rm s}48'59''.0$.

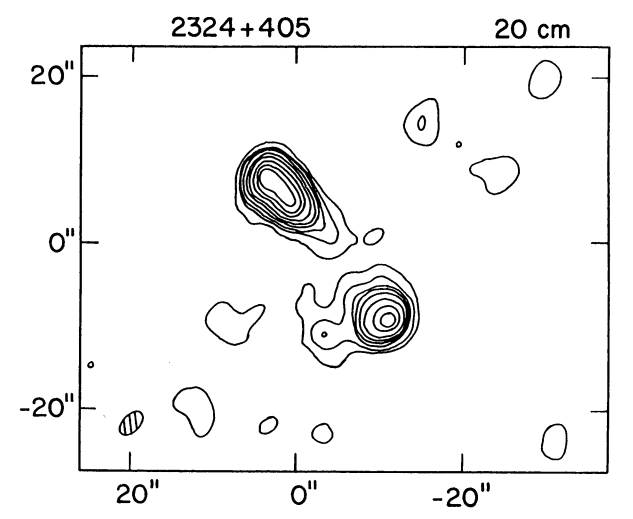


FIG. 1(v). Source: 2324 + 405; taper: 15 km; peak flux: 0.44 Jy; offsets from $\alpha = 23^{\rm h}24^{\rm m}30^{\rm s}69$, $\delta = +40^{\rm s}31^{\rm s}38^{\rm s}0$.

TABLE V. Galactic or suspected galactic sources omitted from complete sample.

0525 - 127	0716-131	
0539-019	1711 - 384	
0605 - 063	1727 — 212	
0702 - 103	1730 — 328	
0707 — 184	1831 - 21	

obtained from the literature that is listed in the Appendix. After tabulating all published data on the structures of the 444 objects, we were left with a total of 18 sources for which high-resolution observations had not been made; these sources are listed in Table VI. Most of the 18 objects, which include three galaxies, ten quasars, and five unidentified sources, are located below the celestial equator. They are used in the parts of our analysis which do not rely on source structure but are removed from the sample when we consider structure-dependent parameters (e.g., linear size). Since the 18 objects represent less than 5% of the complete sample, we are confident that inclusion of their structures would not significantly change the conclusions of this paper.

b) Distribution of Spectral Indices

Two-point spectral indices have been derived for the 444 sources in the complete sample. Whenever possible, we have computed spectral indices between 1480 and 4900 MHz (or 1465 and 4885 MHz) from our VLA data. In \sim 15 cases, sources were so heavily resolved that our lack of short spacings caused the VLA measurements to underestimate the total flux, particularly at the higher frequency. For these objects and for all other sources in our sample, spectral indices between 2.7 and 5 GHz (first choice) or 5 and 10.7 GHz (second choice) were computed using flux densities taken from the references specified in Table IX. The distribution of spectral indices in various categories is shown in Table VII and in Figs. 2(a)-2(d). In our total source sample, we find median spectral indices which are, within the errors, the same as those found by Pauliny-Toth et al. (1978). This

TABLE VI. Extragalactic sources with unknown structure.

0119+115	0605 - 085	
0157 - 311	0646 - 306	
0201 - 440	0648 - 165	
0400 - 319	1144 - 379	
0402 - 362	1313 — 333	
0413 - 210	1459 - 419	
0446 + 112	1543 + 005	
0451 - 282	1947 + 079	
0511 - 220	2223 + 210	
	· ·	

agreement occurs separately for quasars, for galaxies, and for unidentified objects. The distribution of spectral indices also has the characteristic shape found previously, with a narrow peak at $\alpha \simeq -0.7$, caused mostly by radio galaxies, superimposed on a much broader distribution peaking near $\alpha \simeq -0.1$ and caused mostly by quasars. Since we are working from a sample of sources which is essentially a high flux density subset of the Pauliny-Toth *et al.* sample, this result encourages us to believe that the use of several different spectral indices has introduced no systematic bias in our study.

Our improvement on earlier work is our ability to consider resolved and unresolved sources at the one-arcsecond level separately for such a large sample. We find the unsurprising result that resolved sources have much steeper spectra than do unresolved objects. Of particular interest is the fact that both unresolved and resolved quasars have flatter spectra than those possessed by unresolved radio galaxies. As we will show in Sec. III c, resolved quasars do have a relatively high percentage of their total flux density in the compact central component, accounting in part for their flat spectra. But the fact that the 26 completely unresolved radio galaxies have steeper spectra (median $\alpha = -0.40$) than the 77 resolved quasars (median $\alpha = -0.28$) is rather striking. It implies that the unresolved galaxies are less likely than quasars of all types to have a substantial fraction of their flux in a self-absorbed central component. For this reason, we suspect that many of the currently unresolved radio galaxies would be resolved on scales of ~ 0 "1, very much larger than the apparent sizes of the

TABLE VII. Distribution of two-point spectral index for complete sample.

	Total sample Median		Resolved Median		Unresolved Median		Unknown Median	
Source type	index	No.	index	No.	index	No.	index	No.
Il sources in sample				-				
ll sources alaxies SO nidentifed	- 0.40 - 0.76 - 0.08 - 0.55	444 157 230 57	$\begin{array}{c} -0.73 \\ -0.80 \\ -0.28 \\ -0.77 \end{array}$	229 128 77 24	- 0.09 - 0.40 - 0.02 - 0.33	197 26 143 28	0.11 0.1 0.3	18 3 10 5
ources surveyed by VLA								
ll sources alaxies SO nidentified	- 0.22 - 0.65 - 0.07 - 0.55	290 57 184 49	- 0.59 - 0.76 - 0.20 - 0.76	99 32 46 21	- 0.10 - 0.38 - 0.03 - 0.33	191 25 138 28		

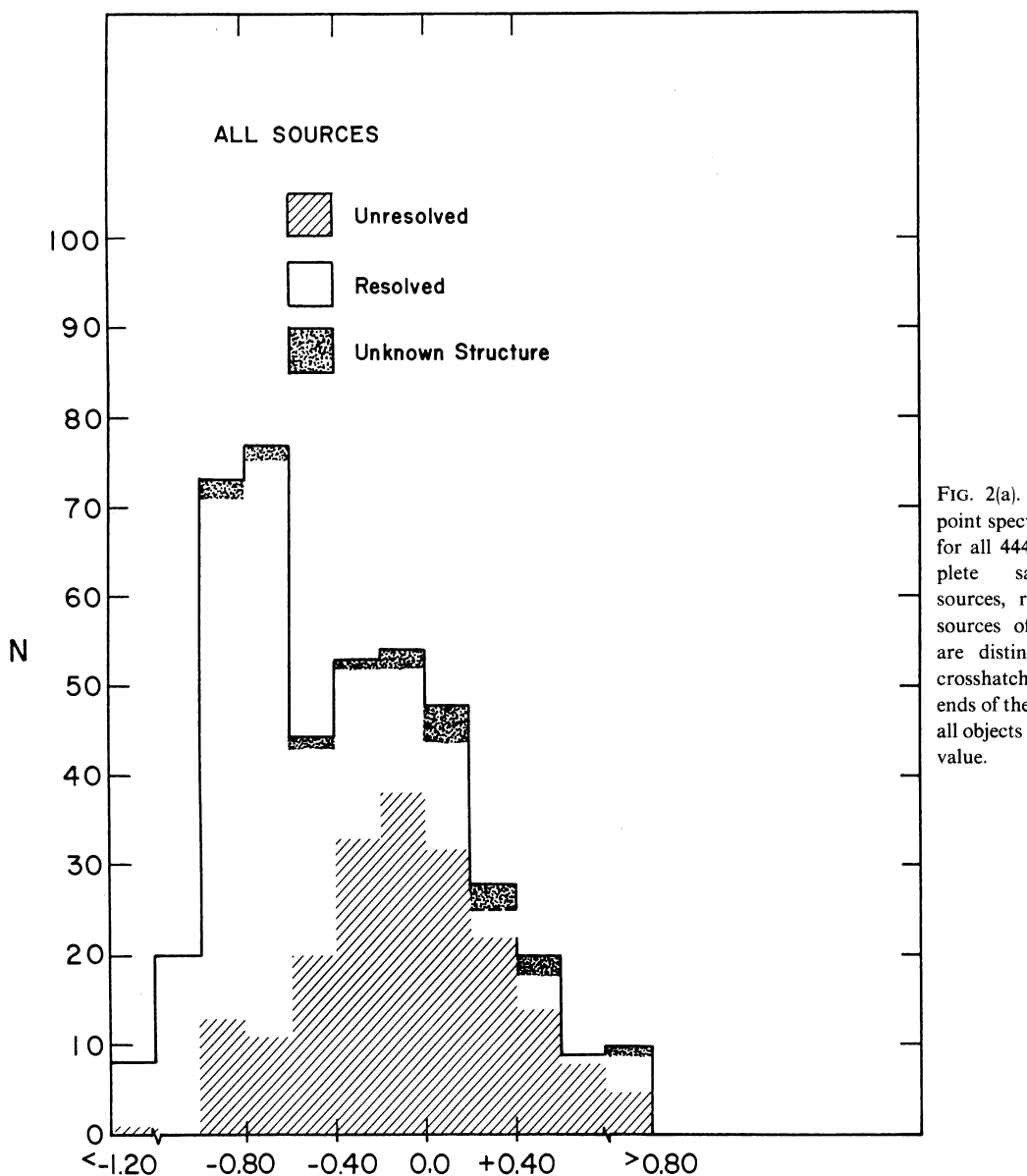


FIG. 2(a). Distribution of two-point spectral index, α $(S_{\nu} \propto \nu^{\alpha})$, for all 444 sources in the complete sample. Unresolved sources, resolved sources, and sources of unknown structure are distinguished by different crosshatching. Note that the ends of the horizontal axes show all objects with α beyond a given value

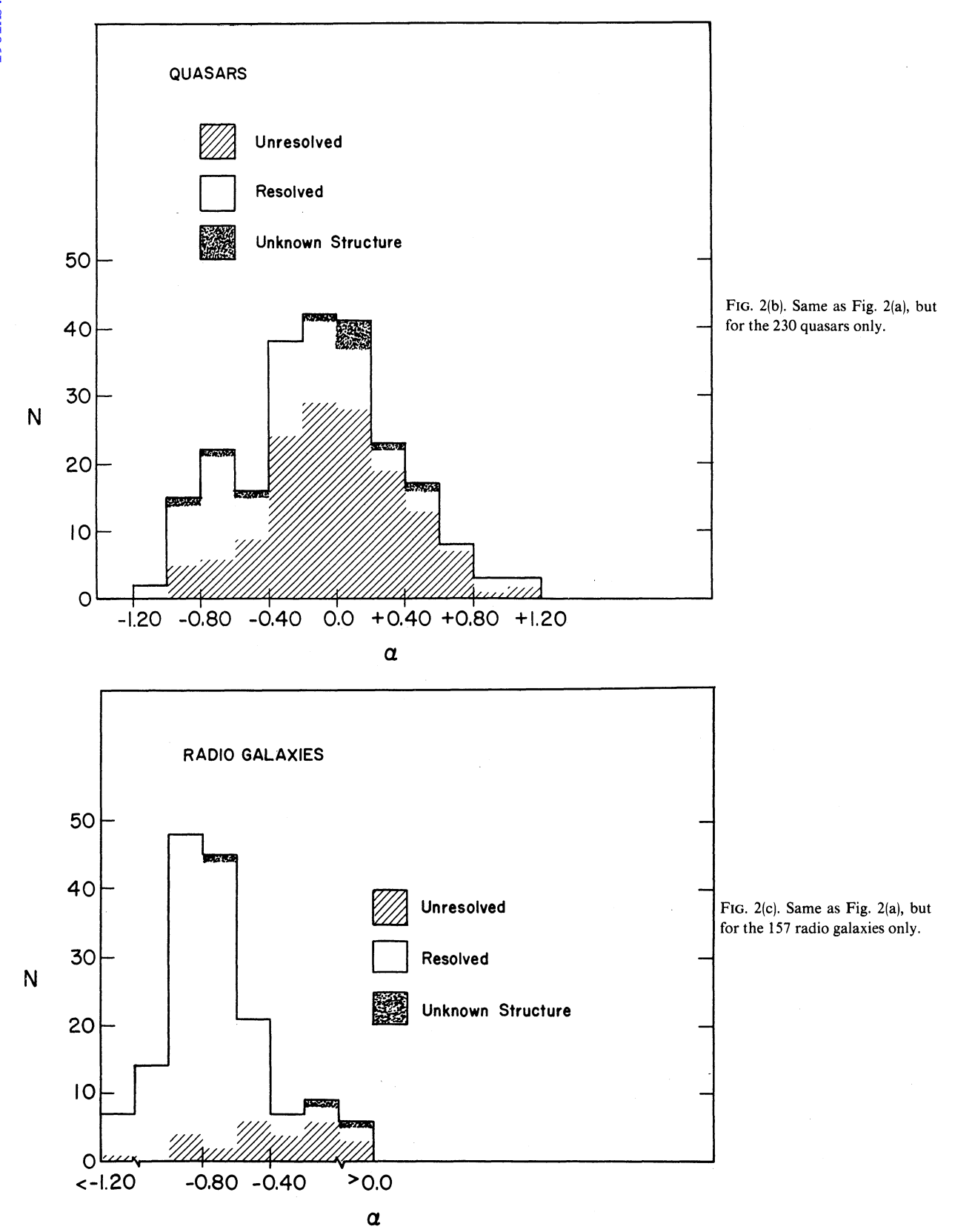
compact components of quasars observed in very long baseline studies (e.g., Pearson, Readhead, and Wilkinson 1980).

The histogram of spectral indices for optically unidentified sources mimics the total distribution of spectral indices fairly well. This subset of our sample may have a larger percentage of radio galaxies than does the subset containing optically identified objects (~40%). The breakdown into resolved and unresolved sources makes it seem that almost all the unidentified objects could be radio galaxies; however, this result is somewhat misleading, owing to the fact that four of the six unidentified sources of unknown structure (the "ultra-mysterious" sources) have inverted spectra and could all be quasars.

Finally, a comparison of the total sample with the subset of sources observed with the VLA shows that the latter sources have spectra slightly flatter than the average. We attribute this effect to the fact that most previously resolved sources were not re-observed with the VLA. Therefore our VLA sample is more heavily weighted by unresolved sources (66% vs 46% in the complete sample) and quasars (76% of the identified sources vs 59% in the complete sample).

c) Source Structure

Figure 3 displays the number of sources versus linear size of the radio source for those objects in the complete sample having measured redshifts and known structure



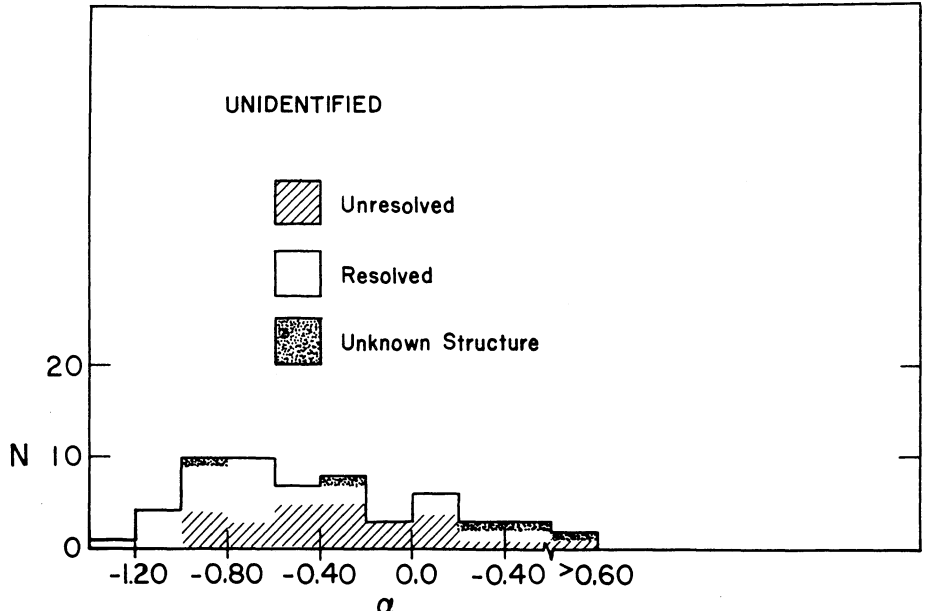


FIG. 2(d). Same as Fig. 2(a), but for 57 unidentified sources only.

(references in Table IX). The sizes have been computed in a cosmological model having $H_0=75\,\mathrm{km\,s^{-1}\,Mpc^{-1}}$ and $q_0=0.1$, using formulas given by Peebles (1971) and Sciama (1971), and have been binned in intervals of size 50 kpc. For radio galaxies, the median size appears to be $\sim 100\,\mathrm{kpc}$. On the other hand, almost all radio sources in quasars are less than 100 kpc in diameter. In fact, the majority of the quasars are unresolved and have apparent sizes of less than 10 kpc, whereas only $\sim 10\%$ of the radio galaxies with known redshifts are unresolved.

A total of 99 of the resolved sources in the complete sample were observed at the VLA. Figures 4(a)-4(c) plot the distribution of these sources as a function of the percentage of the 1480-MHz flux density found in the unresolved component. We do not consider all resolved sources (including those not observed at the VLA) in this histogram, owing to the different beam sizes in the published data. From the figure, it is apparent that the resolved quasars tend to be dominated by the core flux density (36 of 46 have more than 50% of their flux density in the compact component), whereas extended emission dominates the resolved radio galaxies (only ten of 32 have more than half their flux density in the unresolved component). The resolved, optically unidentified sources have the majority of their flux density in the compact component in 15 of 21 cases. In this respect, the unidentified sources appear to resemble quasars. However, as we have noted in Sec. III b, their spectral indices are distributed quite similarly to those of radio galaxies.

Only 11 of the 26 unresolved radio galaxies in the complete sample have known redshifts. In contrast, 94 of the 131 resolved galaxies have measured redshifts. We are unable to evaluate the importance of selection effects in this difference; for example, optical astrono-

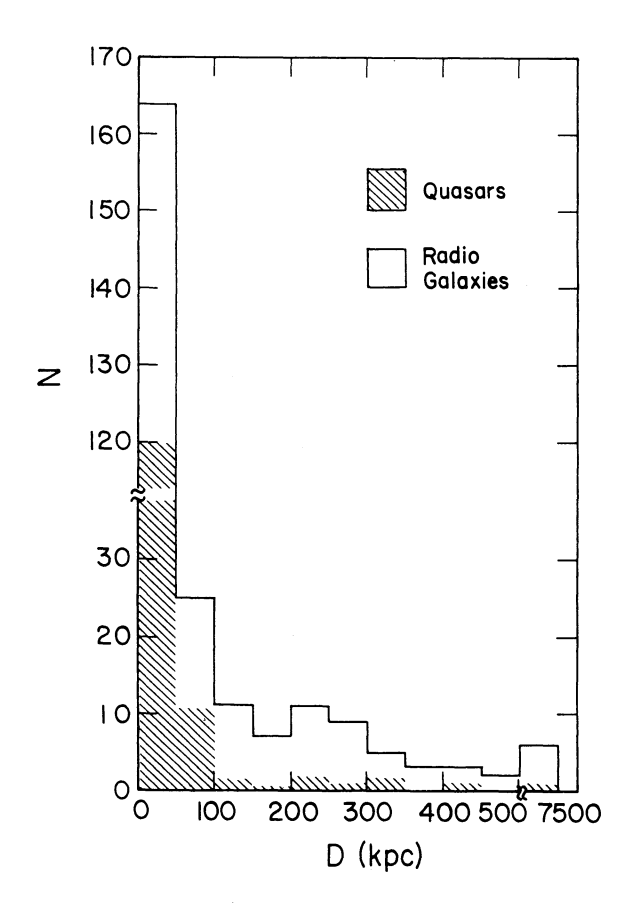


FIG. 3. Distribution of linear sizes for all sources in the flux-limited sample having measured redshifts. This plot includes 87 unresolved quasars and 12 unresolved radio galaxies (note the break in the scale for sources less than 50 kpc in diameter).

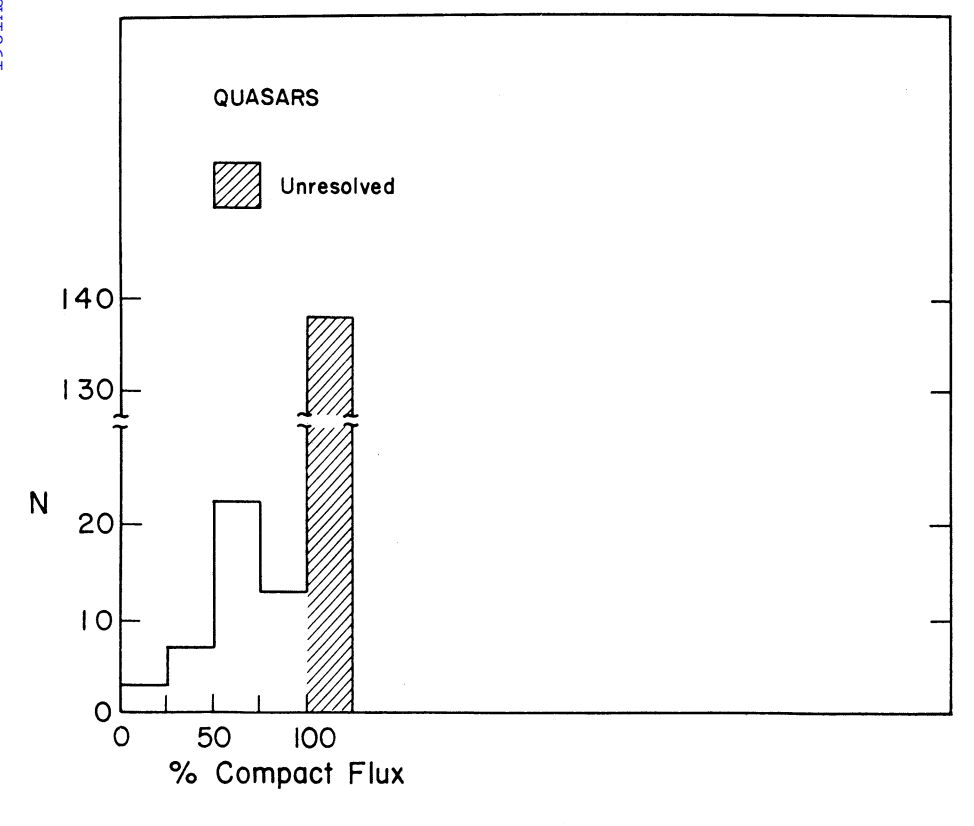


FIG. 4(a). Percentage of total radio flux in the strongest unresolved component at λ 20 cm for the quasars in the complete sample observed at the VLA. The crosshatched portion on the right side of the histogram indicates the unresolved sources (note the break in the scale for unresolved quasars).

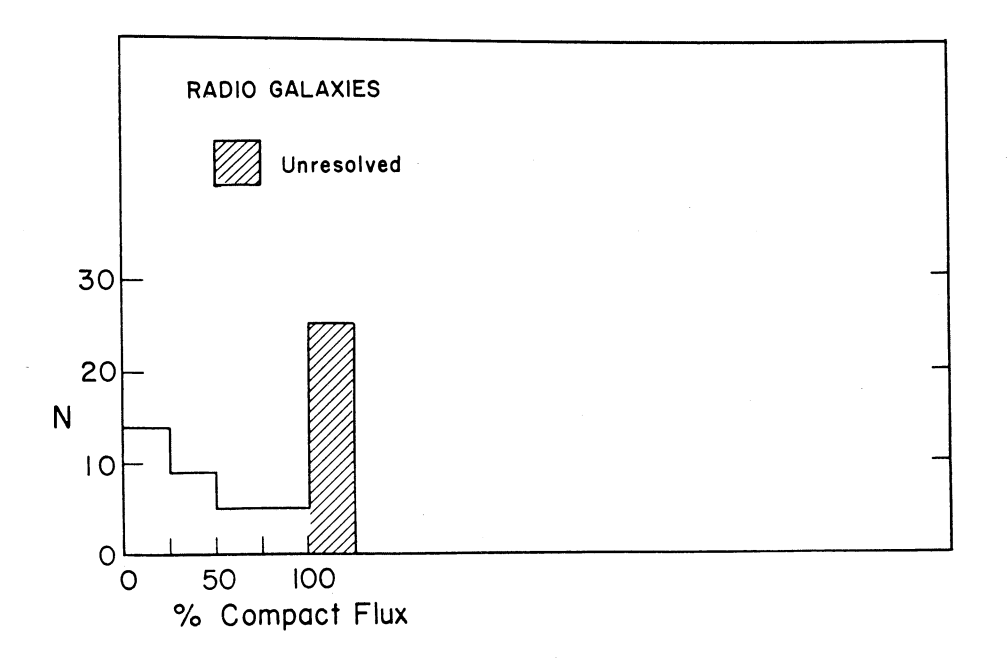


FIG. 4(b). Same as Fig. 4(a), but for radio galaxies.

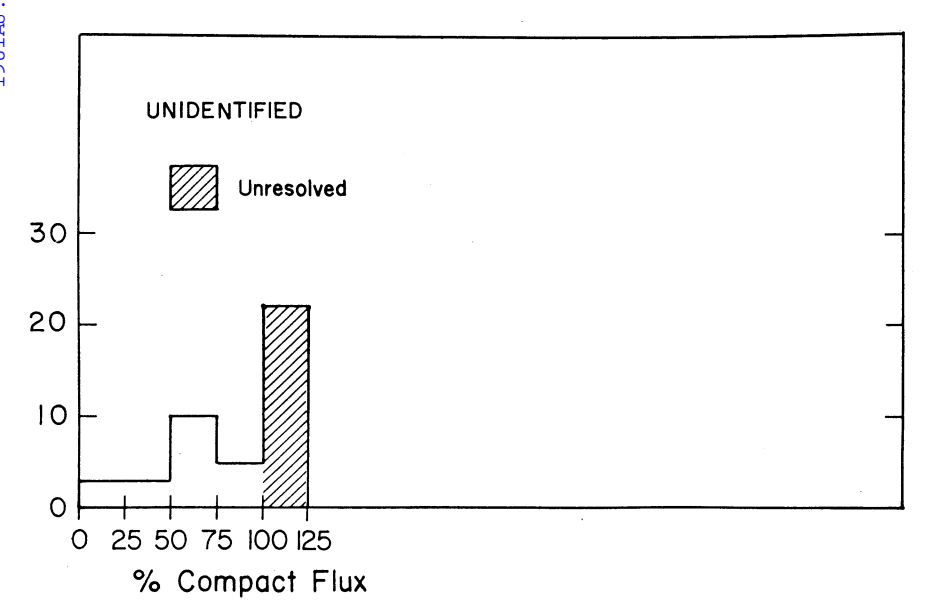


FIG. 4(c). Same as Fig. 4(a), but for unidentified sources.

mers may prefer to measure redshifts for radio galaxies already well known to be resolved sources rather than for objects of undetermined or unresolved structure. Nevertheless, we do note that the median apparent magnitude for the resolved galaxies is $V = 17^{m0}$, while the similar number for unresolved galaxies is $V = 19^{m}0$, with 20 of the 26 unresolved galaxies being fainter than V = 17^m0. This implies that fewer of the unresolved radio galaxies have measured redshifts because they are optically fainter than the resolved galaxies, and thus have a higher ratio of radio to optical luminosity. This luminosity ratio suggests the possibility that the unresolved galaxies are more distant and could be strong radio sources because their radio emission is enhanced by relativistic beaming (e.g., Scheuer and Readhead 1979). A similar effect might cause the high percentage of the flux density in the compact component of unidentified sources, as noted above.

The radio morphology of quasars and radio galaxies has been discussed by Fanti and Padriella (1977), Owen, Porcas, and Neff (1978), Miley and Hartsuijker (1978), and others. Fanti et al. (1977) present the structure of B2 quasars as being (a) extended sources, (b) double or triple sources with the central source coinciding with the optical image of the quasar, or (c) asymmetrical double sources or D2 quasars such as 3C 273. We also see such structures in the quasars observed at the VLA. In addition, the well resolved radio galaxies usually show classical double or triple structure, as expected.

Inspection of all the new maps of the sources observed at the VLA shows that in over one-third of the sources, the type of structure is not well determined by our limited *u-v* coverage. Thus the statistics on detailed morphology gleaned from the sources with good VLA maps may

not be representative of the entire list of 229 resolved sources in the complete sample, so we have not attempted to derive such statistics. A study of Table IV and Figs. 1(a)-1(v) shows that, although there may be one or

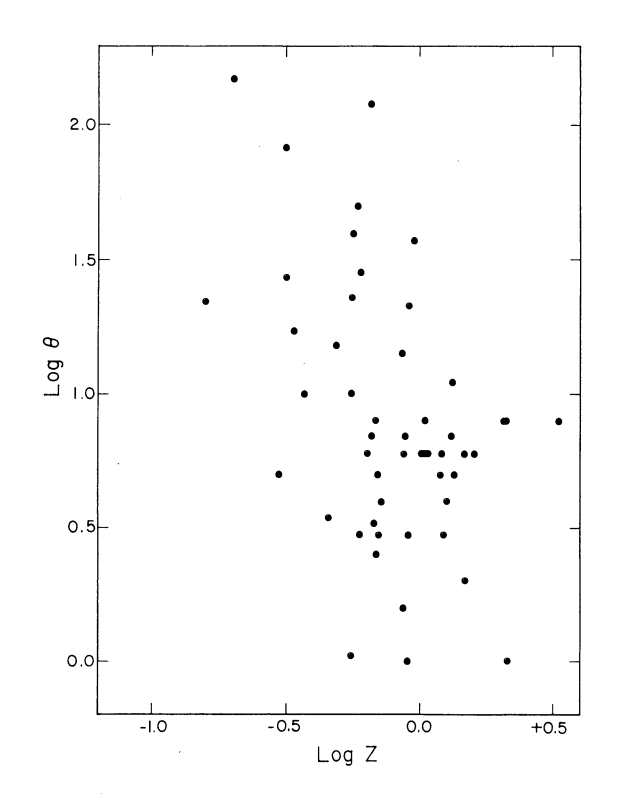


Fig. 5(a). Plot of θ (largest angular size) vs z for the resolved quasars in the complete sample.

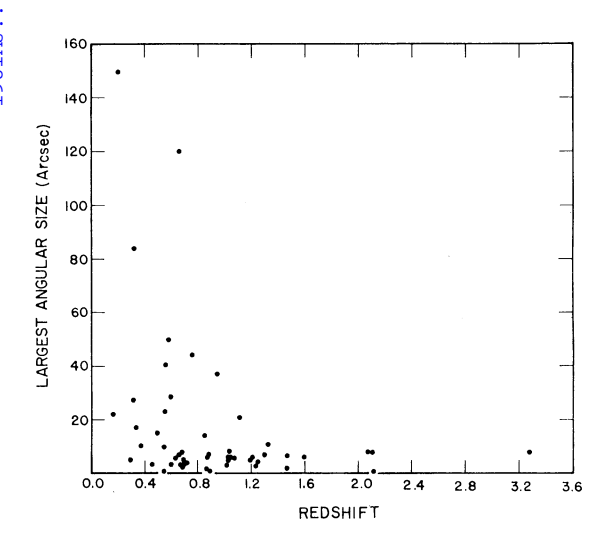


FIG. 5(b). Same as Fig. 5(a), but on a linear scale (unresolved sources omitted).

two dominant components, there is often considerable flux density in either another component or extended structure; in a few cases, some of the extra flux may be in high sidelobes caused by the limited u-v coverage.

d) θ-z Diagram

We have graphed the complete sample's resolved quasars in a linear plot of θ vs z [Fig. 5(a)], where θ represents the largest angular size present in the source. Figure 5(b) is a plot of largest angular size vs z on a linear scale rather than a logarithmic scale. A total of 51 quasars have both measured redshifts and angular sizes $\gtrsim 1$ arcsec. The unresolved quasars, all of which have sizes < 1 arcsec, have been omitted from the diagrams. Our plot of θ vs z looks similar to that of Wardle and Miley (1974), whose sample of quasars was predominantly selected from the Cambridge low-frequency radio surveys. We find no well defined minimum in the angular size distribution, implying that the evolutionary effects are important for our high-frequency selected quasars. We note that selection effects caused by our flux-limited sample may be important. However, it does seem that the linear sizes of the radio sources in high-redshift qua-

TABLE VIII. Resolved quasars as a function of redshift.

$\log\!Z$	Quasars	Unresolved	Resolved	Fraction resolved (%)
< - 0.5	12	7	5	42
-0.5 to -0.3	14	9	5	36
-0.3 to -0.1	31	14	17	55
-0.1 to $+0.1$	39	23	16	41
+ 0.1 to 0.3	23	18	5	22
> +0.3	19	15	4	21

TABLE IX. References to previously published data.

A. Surveys
1. S surveys
Pauliny-Toth and Kellermann (1972)
Pauliny-Toth et al. (1972)
Pauliny-Toth et al. (1978)
2. Parkes lists
Bolton and Shimmins (1973)
Bolton, Shimmins, and Wall (1975)
Savage, Bolton, and Wright (1977)
Shimmins and Bolton (1972)
Shimmins and Bolton (1974)
Shimmins, Bolton, and Wall (1975)
Shimmins, Manchester, and Harris (1969)
Wall, Shimmins, and Merkelijn (1971)
Wall et al. (1976)
B. Optical data (identifications, magnitudes, redshifts)
Burbidge and Crowne (1979)
Burbidge, Crowne, and Smith (1977)
Hewitt and Burbidge (1980)
Kühr et al. (1980)
Veron and Veron 1974 (1977 update).
In addition, optical data were taken from the surveys listed in Part
A of this table and occasionally from radio structure papers listed in Part D.
C. Radio flux densities
The primary sources of flux densities were the surveys listed in Part
A. Flux densities of VLA calibrators came from the VLA calibration list (Formalist and Parlay). Additional information game from the
list (Fomalont and Perley). Additional information came from the
following references:
Bell, Seaquist, and Braun (1971)
Kellermann and Pauliny-Toth (1973)
Kühr <i>et al.</i> (1980)
D. Radio structures
Bash (1968)
Branson <i>et al.</i> (1972)
Bridle et al. (1972)
Bridle, Kesteven, and Brandie (1977)
Donaldson, Miley, and Palmer (1971)
Ekers (1969)
Fomalont (1971)
Högbom and Carlsson (1974)
Jenkins, Pooley, and Riley (1977)
Longair (1975)
Macdonald, Kenderdine, and Neville (1968)
Macdonald and Miley (1971)
Mackay (1969)
Miley and van der Laan (1973)
Mitton (1970)
Owen, Porcas, and Neff (1978)
Pacholczyk (1978)
Perley, Fomalont, and Johnston (1980)
Perley, Fomalont, and Johnston (1981)
Perley and Johnston (1979)
Pooley and Henbest (1974)
Potash and Wardle (1979)
Riley and Pooley (1975)
Schilizzi and Ekers (1975)
Schilizzi and McAdam (1975)
Stull et al. (1975)
Wall and Cole (1973)
Womisk (1077)

Wraith (1972) The Parkes lists also contain information on the structures of some sources; in addition, the VLA calibrator list was used extensively.

Warwick (1977)

Weiler and Johnston (1980) Wilkinson (1972) Wills (1975)

sars are not the same as for low-redshift quasars. As is evident from Fig. 5(b), quasars having z > 1 tend not to have radio sources with large linear diameters. Table VIII shows that these most distant quasars are much less likely to be associated with resolved radio sources

than are their more nearby cousins, a fact not attributable to an increased linear diameter of the telescope beam for sources of increasing distance. This could indicate that the effects of relativistic beaming are important for very luminous quasars, in that we see *no* large radio sources in the distant, highly luminous quasars because their brightness has been enhanced by beams directed very close to our line of sight. A more complete discussion of possible origins of the redshift dependence is given by Wardle and Miley (1974).

IV. SUMMARY

A flux-limited sample of strong 5-GHz extragalactic radio sources has been studied using new VLA observations and data in the literature. This study shows that the compact quasars and radio galaxies (size $\leqslant 1''$) have a median spectral index of $\alpha=-0.09$ at centimeter wavelengths, whereas sources which display resolved structure (> 1'') have a median spectral index of $\alpha=-0.73$. The spectra of unresolved radio galaxies are shown to be steeper than those of both the unresolved and the resolved quasars; the comparison with the resolved quasars shows that even these extended quasars are more likely to have a substantial flux density contribution from a self-absorbed central component than are the compact sources in radio galaxies.

About two-thirds of the quasars in the complete sam-

ple are unresolved at the arcsecond level, while less than 20% of the radio galaxies are unresolved (see Table VII). The structures displayed by the resolved sources are in agreement with those found in earlier studies. There is evidence for a dearth of large radio sources in quasars beyond $z \simeq 1$. One possible interpretation of this result is relativistic beaming of radiation from compact radio sources, since there are no large radio sources among the very luminous quasars observed at great (z > 1) distances.

APPENDIX

We drew information from many different references for this paper. We have compiled data on each of the 444 individual radio sources in our complete list of extragalactic objects stronger than 1 Jy at 5 GHz. That information has been used to derive the figures and tables which refer to our complete sample. However, for reasons of space, we have chosen not to publish the entire compilation on a source-by-source basis. Instead, the relevant data for the complete sample are shown in figures throughout this paper. Appropriate information about the sources we have observed at the VLA is given in Tables III and IV. References for various categories of data in these tables and in our larger compilation are given in Table IX.

REFERENCES

Baars, J. W. M., Genzel, R., Pauliny-Toth, I. I. K., and Witzel, A. (1977). Astron. Astrophys. 61, 99.

Bash, F. N. (1968). Astrophys. J. Suppl. 16, 373.

Bell, M. B., Seaquist, E. R., and Braun, L. D. (1971). Astron. J. 76, 524.

Bolton, J. G., and Shimmins, A. J. (1973). Aust. J. Phys. Astrophys. Suppl., No. 30.

Bolton, J. G., Shimmins, A. J., and Wall, J. V. (1975). Aust. J. Phys. Astrophys. Suppl., No. 34.

Branson, N. J. B. A., Elsmore, B., Pooley, G. G., and Ryle, M. (1972).Mon. Not. R. Astron. Soc. 156, 377.

Bridle, A. H., Davis, M. M., Fomalont, E. B., and Lequeux, J. (1972).

Astron. J. 77, 405.

Bridle, A. H., Kesteven, M. J. L., and Brandie, G. W. (1977). Astron. J. 82, 21.

Burbidge, G. R., and Crowne, A. H. (1979). Astrophys. J. Suppl. 40, 583.

Burbidge, G. R., Crowne, A. H., and Smith, H. E. (1977). Astrophys. J. Suppl. 33, 113.

Donaldson, W., Miley, G. K., and Palmer, H. P. (1971). Mon. Not. R. Astron. Soc. 152, 145.

Ekers, J. A. (1969). Aust. J. Phys. Astrophys. Suppl., No. 7.

Fanti, C., Fanti, R., Formiggini, L., Lari, C., and Padrielli, L. (1977).
Astron. Astrophys. Suppl. 28, 351.

Fanti, R., and Padrielli, L. (1977). Astron. Astrophys. Suppl. 29, 263. Fomalont, E. B. (1971). Astron. J. 76, 513.

Hewitt, A., and Burbidge, G. (1980). Astrophys. J. Suppl. 43, 57.

Högbom, J. A., and Carlsson, I. (1974). Astron. Astrophys. 34, 341.

Jenkins, C. J., Pooley, G. G., and Riley, J. M. (1977). Mem. R. Astron. Soc. 84, 61.

Kellermann, K. I., and Pauliny-Toth, I. I. K. (1973). Astron. J. 78, 828.

Kühr, H., Nauber, U., Pauliny-Toth, I. I. K., and Witzel, A. (1980).

Preprint.

Longair, M. S. (1975). Mon. Not. R. Astron. Soc. 173, 309.

Macdonald, G. H., Kenderdine, S., and Neville, A. C. (1968). Mon. Not. R. Astron. Soc. 138, 259.

Macdonald, G. H., and Miley, G. K. (1971). Astrophys. J. **164**, 237. Mackay, C. D. (1969). Mon. Not. R. Astron. Soc. **145**, 31.

Miley, G. K., and Hartsuijker, A. P. (1978). Astron. Astrophys. Suppl. 34, 129

Miley, G. K., and van der Laan, H. (1973). Astron. Astrophys. 28, 359. Mitton, S. (1970). Mon. Not. R. Astron. Soc. 149, 101.

Owen, F. N., Porcas, R. W., and Neff, S. G. (1978). Astron. J. 83, 1009. Pacholczyk, A. G. (1978). A Handbook of Radio Sources: Book 1 (Pachart, Tucson).

Pauliny-Toth, I. I. K., and Kellermann, K. I. (1972). Astron. J. 77, 797.

Pauliny-Toth, I. I. K., Kellermann, K. I., Davis, M. M., Fomalont, E. B., and Shaffer, D. B. (1972). Astron. J. 77, 265.

Pauliny-Toth, I. I. K., Witzel, A., Preuss, E., Kühr, H., Kellermann, K. I., Fomalont, E. B., and Davis, M. M. (1978). Astron. J. 83, 451.
Pearson, T. J., Readhead, A. C. S., and Wilkinson, P. N. (1980). Astrophys. J. 236, 714.

Peebles, P. J. E. (1971). *Physical Cosmology* (Princeton University, Princeton).

- 85, 649.
- Perley, R. A., Fomalont, E. B., and Johnston, K. J. (1980). Astron. J.
- Perley, R. A., Fomalont, E. B., and Johnston, K. J. (1981). In preparation.
- Perley, R. A., and Johnston, K. J. (1979). Astron. J. 84, 1247.
- Pooley, G. G., and Henbest, S. N. (1974). Mon. Not. R. Astron. Soc. 169, 477.
- Potash, R. I., and Wardle, J. F. C. (1979). Astron. J. 84, 707.
- Riley, J. M., and Pooley, G. G. (1975). Mem. R. Astron. Soc. 80, 105. Savage, A., Bolton, J. G., and Wright, A. E. (1977). Aust. J. Phys. Astrophys. Suppl., No. 44.
- Scheuer, P. A. G., and Readhead, A. C. S. (1979). Nature 277, 182.
- Schilizzi, R. T., and Ekers, J. A. (1975). Astron. Astrophys. 40, 221.
- Schilizzi, R. T., and McAdam, W. B. (1975). Mem. R. Astron. Soc. 79,
- Sciama, D. W. (1971). Modern Cosmology (Cambridge University, Cambridge).
- Shimmins, A. J., and Bolton, J. G. (1972). Aust. J. Phys. Astrophys. Suppl., No. 23.
- Shimmins, A. J., and Bolton, J. G. (1974). Aust. J. Phys. Astrophys.

- Suppl., No. 32.
- Shimmins, A. J., Bolton, J. G., and Wall, J. V. (1975). Aust. J. Phys. Astrophys. Suppl., No. 34.
- Shimmins, A. J., Manchester, R. N., and Harris, B. J. (1969). Aust. J. Phys. Astrophys. Suppl., No. 8.
- Stull, M. A., Prince, K. M., D'Addario, L. R., Wernecke, S. J., Graf, W., and Grebenkemper, C. J. (1975). Astron. J. 80, 559.
- Veron, M. P., and Veron, P. (1974). Astron. Astrophys. Suppl. 18, 309. Wall, J. V., Bolton, J. G., Wright, A. E., Savage, A., and van der Hagen, J. (1976). Aust. J. Phys. Astrophys. Suppl., No. 39.
- Wall, J. V., and Cole, D. J. (1973). Aust. J. Phys. 26, 881.
- Wall, J. V., Shimmins, A. J., and Merkelijn, J. K. (1971). Aust. J. Phys. Astrophys. Suppl., No. 19.
- Wardle, J. F. C., and Miley, G. K. (1974). Astron. Astrophys. 30, 305. Warwick, R. S. (1977). Mon. Not. R. Astron. Soc. 179, 1.
- Weiler, K. W., and Johnston, K. J. (1980). Mon. Not. R. Astron. Soc.
- Wilkinson, P. N. (1972). Mon. Not. R. Astron. Soc. 160, 305.
- Wills, B. J. (1975). Aust. J. Phys. Astrophys. Suppl., No. 38.
- Wraith, P. K. (1972). Mon. Not. R. Astron. Soc. 160, 283.